2018 SAE Design Report

University of Tulsa

Regular Class

Team Members:

Kelly Shelts - Team Leader

Jarrod Braun

Garrett Carson

Duy Van

Fahad Ansari

Ryan Ogilvie

Hossam Dawood

Othman Al-Yousef

Glenn Lane

Faculty Advisor

Dr. Jim Sorem

Table of Contents Page Number

Appendix

List of Figures and Tables

Statement of Purpose

The team was to design, build, and test an RC plane to compete in the Society of Automotive Engineers Aero Design Competition in the Regular Class. The plane's purpose was to carry as many passengers and cargo (tennis balls and metal weights) as possible given several design constraints. The final design and report were delivered to SAE March 1 and the team took the plane to competition April 6-8.

1.0 Executive Summary

The SAE Aero Design Challenge is an international collegiate competition in which students compete to design, manufacture, test, and fly remote controlled airplanes to score points. The regular class competition simulates real life challenges by requiring the aircraft to carry both passengers and cargo, represented by tennis balls and weights. The goal of the competition is to carry the largest amount of passengers and cargo given several design constraints. The competition design requirements are shown below in Table 1.0.1.

Table 1.0.1 Competition Design Requirements

Wattage	<1000 Watts	**Flight Circuit**	1 Loop
Wingspan	<12 ft	**Max Plane and Cargo Weight**	55 Pounds
Battery	22.2V Lithium Polymer, Min 3000 mah	**Motor**	Electric
Takeoff	< 200 ft	**Materials**	No Fiber reinforced plastics

The 2018 TU plane utilizes a single 12 foot long backward swept wing, a 10 foot long fuselage, and a tail section consisting of horizontal and vertical stabilizers. The plane was designed to be as light as possible, while still being able to carry as much weight as possible. Iterative design and analysis was performed to maximize performance, the results of which are shown in Table 1.0.2. The strategy for this season was to build a reliable plane with exchangeable parts so that it can complete each round. This is done by optimizing airframe design to maximize lift, minimize drag, and reduce the weight of the plane so as to maximize the number of passengers and cargo loads that can be carried. Test flights of this

year's plane were also successfully performed prior to design submission in order to verify the predictions shown in Table 1.0.2.

Table 1.0.2 Projected Performance

Plane Weight	17.3 lbs
Wing area	19.2 ft^2
Max weight	31.7 lbs
Carried weight	13.8 lbs
Score	68.7

However, due to transmitter issues, the plane suffered from two crashes at the competition, which leads into future recommendations for the project. Heavy transmitter range testing is recommended as it is a critical component of an RC plane to be able to respond to pilot inputs and prevent accidents. Wiring, battery capacity tests along with multiple test flights are recommended for the next generation of Aero plane in order to make sure the plane is in flyable condition at the competition. Despite these issues, the two customers, SAE and The University of Tulsa were satisfied as the plane passed safety inspections and scored well at the competition.

The TU SAE Aero team is unusual in that TU does not have an aerospace engineering program and all students on the team study mechanical engineering. Most other This provides an additional challenge that has motivated the team to do extra research and testing to learn about aerodynamic and airplane structural principles in order to be as competitive as possible.

2.0 Schedule Summary

In order to complete this task, design work started in Fall 2017, shown below in Figure 2.0.1.

	September 25-October 1	October 2- 8	October 9-15	October 16-22	October 23-29	October 30-November 5	November 6 - 12	November 13-19	November 20-26	November 27-Dec 3
Test Fly 2017 Plane										
Air Frame Design (CFD)										
Structural Design Brainstorming										
Research Vendors										
Propeller and Motor Test										
Solidworks										

Figure 2.0.1: Fall 2017 Schedule

A spring semester schedule is shown below in Figure 2.0.2.

	Jan 8-14	Jan 15-21	Jan 22-28	Jan 29-Feb 4	Feb 5-11	Feb 12-18	Feb 19-25	Feb 26-Mar 4	Mar 5-11	Mar 12-18	Mar 19-25	Mar 26-Apr 1
Finish Structural Design												
Structural Analysis												
Order Parts												
Build Frame												
Cover Frame												
Install Electronics												
Test Flight												
Repairs, Improvements												
Write Report												
Create Presentation												
Practice Presentation												
Build Spare Parts												

Figure 2.0.2 Spring 2018 Schedule

3.0 Budget

The material cost is listed in Table 3.0.1. The cost of the materials to build the plane three time is about $5,000, which means each plane costs about $1,600. In comparison with past TU planes, this plane was significantly more expensive, about double the cost of the 2017 plane. This is due to the use of higher quality materials and components, which improved the plane. For example, a lower quality sheeting was used in past years, causing wrinkles, tears, and dimpling, which caused excessive drag at the frontal surface of the wings. This year, higher quality MonoKote and specialized application tools were purchased, reducing problems that arose with the cheaper alternative. A crate was built to ship the plane to California and there was shipping cost for both ways. Hotel, flight tickets, and vehicle rentals were also big factors that significantly contribute to the grand amount that the university actually spent, which was approximately $14,000. On the other hand, if the labor cost was taken into account, the total engineering hours was 1,280, including designing, analyzing, building the plane, and preparing report and presentation. With assumption of $100 per hour for designing and analyzing, and $60 per hour for building and writing report, the estimated labor cost was about $100,800.

Table 3.0.1: Budget

Table 3.0.1 a: Material Cost

Materials	
Items	Costs ($)
Electronic cost	936.4
Structural material cost	2644.85
Monokote, glues, and tools cost	1412.03
Crate material cost	432.06
Materials total cost	$ 5,425.34

Table 3.0.1 b: Competition Trip Cost

Updated Competition Trip	
Items	costs ($)
Hotel	2040.00
9 x Flight tickets	5130.00
Trailer shipping both ways	900.00
Vehicle Rental	408.00
Total	$ 8,478.00

3.0.1 c: Engineering Labor Cost

Engineering Labor	
Tasks	Time (h)
Fluid Analysis	250
Wing Design	100
Fuselage Design	150
Tail Design	50
Landing Design	50
Plane Building	550
Report & Presentation	100
Shipping crate building	30
Total labor cost	$ 100,800.00

Table 3.0.1 d: Grand Total TU Spent

Grand Total Spent	$ 13,903.34

4.0 Fluid Analysis and Airframe Design

4.1 Airfoil Analysis

Wing design begins with choosing an airfoil, the shape of the wing's profile, which determines the wing's lift and drag coefficients (C_L and C_D). The team analyzed five high lift airfoils: the NACA 9312, FX74 CL5, CH10, S1210, and S1223. The foils were analyzed using Computational Fluid Dynamics (CFD) and software XFLR5 using a base chord length of 1 ft . The analysis was run using a constant Reynold's Number of 295,276, calculated using the density of air at sea level and a velocity of approximately 27 mph. and varying angles of attack. Chart 4.1.1 summarizes the findings for comparison.

Table 4.1.1: Airfoil Analysis

Airfoil	**C_L at 0°**	**C_D at 0°**	**C_L/C_D at 0°**	**Max C_L**
NACA 9312	0.844	0.019	44.6	1.5
FX74 CL5	1.09	0.025	41.8	1.62
CH10	0.93	0.024	39.5	1.62
S1210	0.99	0.018	55.7	1.77
S1223	1.11	0.02	55.3	1.84

The Selig 1223 airfoil was chosen for the main wing because it has the highest C_L at an angle of zero degrees, 1.11 It also has the highest maximum C_L of 1.84. Additionally, this foil has a high ratio of C_L/C_D and a low C_D at an angle of attack of zero degrees. However, the S1210 has extremely similar properties. To determine which would actually perform better, two identical wing shapes were simulated using the techniques discussed in Section 4.2, one with the S1223 airfoil and one with the S1210 airfoil. The S1223 wing had a 5% higher weight capacity than the S1210 wing, so the S1223 airfoil was chosen for all further wing simulations and for the final wing design.

4.2 Weight Capacity Analysis Techniques

The team developed a thorough method for determining the weight capacity of the airplane for for both take-off and in-flight conditions. This is crucial for performing well at the competition, since the flight score is dependent on the passenger and luggage capacity of the aircraft. The approach begins with a C_D versus velocity data for a wing with the S1223 airfoil profile, obtained via Computational Fluid Dynamics, show below in Figure 4.2.1.

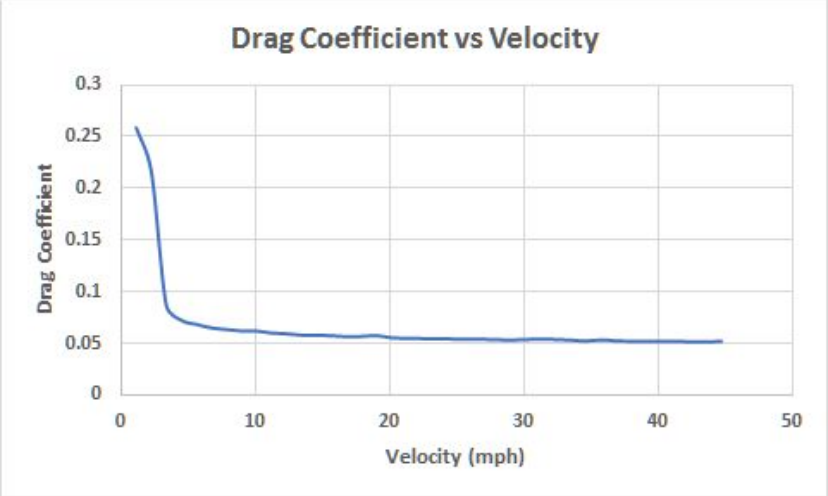

Figure 4.2.1: Generic Graph of Drag Coefficient Versus Velocity

The team wrote a program that creates a piecewise continuous function based on the drag coefficient data obtained from XFLR5. This function changes for each plane tested because each plane has different drag characteristics. Since the drag force D(v) is dependent on the drag coefficient, the following equation can be used to calculate net thrust:

$$T_{net}(v) = T(v) - D(v) - f(v)$$

Where T_{net} (v) is the net force, T(v) is the force of the propeller, D(v) is the drag force, and f(v) is the frictional force. Friction is a function of velocity because as the plane gains speed, lift increases, which reduces the normal force on the wheels from the ground. Acceleration at a specific velocity could then be calculated by dividing the net thrust by the mass of the aircraft. From the kinematic equations of constant acceleration.

$$X = x + vt + 0.5at^2 \qquad \text{and} \qquad V(v) = v + at$$

the distance the plane travels in a very small time increment and its velocity after that time period can be calculated, since acceleration may be considered constant during small time periods. By iterating and summing the distances traveled until takeoff velocity is reached, the total distance the plane travels during takeoff can be calculated. The value for takeoff distance was found to converge to two decimal places when the time increment reached 0.01 seconds.

In order to determine the maximum weight capacity of a wing, the takeoff distance calculator was programmatically repeated with increasing mass values until a takeoff distance of 200 feet was reached. This calculation illustrates the linear relationship between takeoff distance and wing load capabilities.

However, takeoff weight capability is not the same as in flight cargo sustainability. The rotation of the plane on lift-off causes an increase in both lift and drag, which is taken into consideration in the takeoff analysis. However, the plane returns to a low angle of attack during cruising flight, lowering the lift coefficient and requiring a higher speed to maintain sufficient lift. To determine whether a plane is able to achieve the necessary speed, the velocity when the propeller thrust and drag force are equal was calculated. This becomes the maximum speed of the airplane. That velocity is then substituted into the following lift equation to find the maximum weight capacity in-flight, where the lift coefficient is at zero angle of attack:

$$L = \frac{1}{2}\rho v^2 A C_L$$

The lowest value of the takeoff and in-flight weight capacities is taken to be the limiting weight capacity of that wing. These calculations were performed neglecting the added lift from ground effect. This produces more conservative results.

Air properties were assumed to be those at sea level. However, as altitude increases the density of air varies, yielding different weight capacities at different heights. In accordance with the Technical Design Report and Technical Data Sheet requirements, the team captured the payload weight capacity vs altitude for the final design selected. To obtain this information the team calculated pressures and temperatures at various altitudes according to the following two equations:

$$p = p_0\left(1 - \frac{Lh}{T_0}\right)^{\frac{gM}{RL}} \quad \text{and} \quad T = T_0 - Lh$$

where p_0 is the pressure at sea level, L is the temperature lapse rate, h is the altitude, g is acceleration due to gravity, M is the molar mass of air, R is the universal ideal gas constant, and T_0 is the temperature at sea level. Air densities at altitudes ranging from sea level (0 ft) to 4000 ft were then calculated according to the ideal gas law:

$$\rho = \frac{pM}{RT}$$

The limiting weight capacities of the final wing design at those heights were determined based on the corresponding air densities. The results are shown in the appendix.

4.3 Simulations

More than 300 wing designs were simulated to calculate the maximum allowable weight generated using the methods described in Section 4.2. Four different independent variables of the wing design were considered to obtain the allowable weight: wingspan, root chord length, tip chord length,

and taper start location. In order to give a visual of the data, the test points were gathered and presented in different 3D graphs.

Figure 4.3.1 illustrates the wing design simulations for both a rectangular (non-tapered) wing and wings with varying percentage of the middle (largest) chord length as the final (tip) chord length. For the non- taper graph 4.3.1 (a), the root chord is on the horizontal axis, ranges from 12 in to 30 in with 3 in increment and the wingspan is on the depth axis, ranges from 9 to 15 feet with 1 foot increment. The non-taper graph clearly shows that as the wingspan increases from 9 to 15 feet, the maximum allowable weight of the wing also increases. Because of this pattern and the wingspan limitation, the 12 feet wingspan was chosen not only as a fixed variable for the next analysis but also for the final wingspan selection.

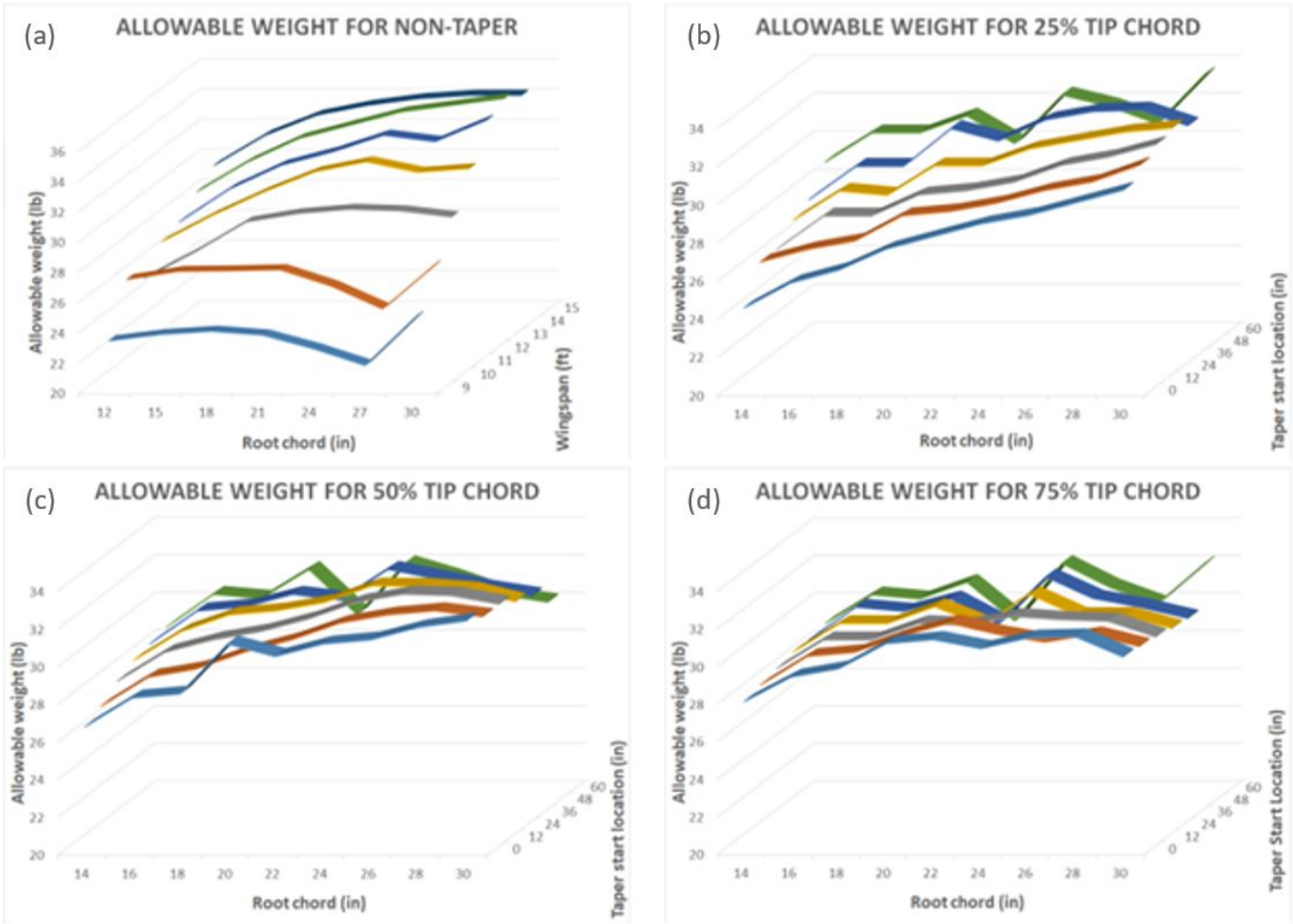

Figure 4.3.1: Allowable Weight for Different Variables

With a constant 12 foot wingspan, there were three independent variables left: tip chord length, root chord, and taper start location. The tip chord lengths considered were 25%, 50%, and 75% of the length of the root chord. A 3D graph was made for each tip chord length ratio, varying root chord length and taper start location to show the allowable weight for each wing. The three graphs are shown in Figure 4.3.1 (b,c,d), which has the same root chord length variable on the horizontal axis, and the taper start location is on the depth axis. The three graphs similarly show that smaller wings with less surface area (smaller root chord length and short taper start location) generate less payload weight. This pattern is more noticeable with smaller tip chord percentage. However, this data cannot solely be used to determine the optimum wing design because as the wings get bigger, they do generate more lift but their own weight also increases as well. Their lifting weight has to compensate for their own weight. As a result, using the four graphs in Figure 4.3.1, net weight graphs were made by subtracting each wing design's allowable weight by their estimated wing weight. The graphs are shown in Fig 4.3.2.

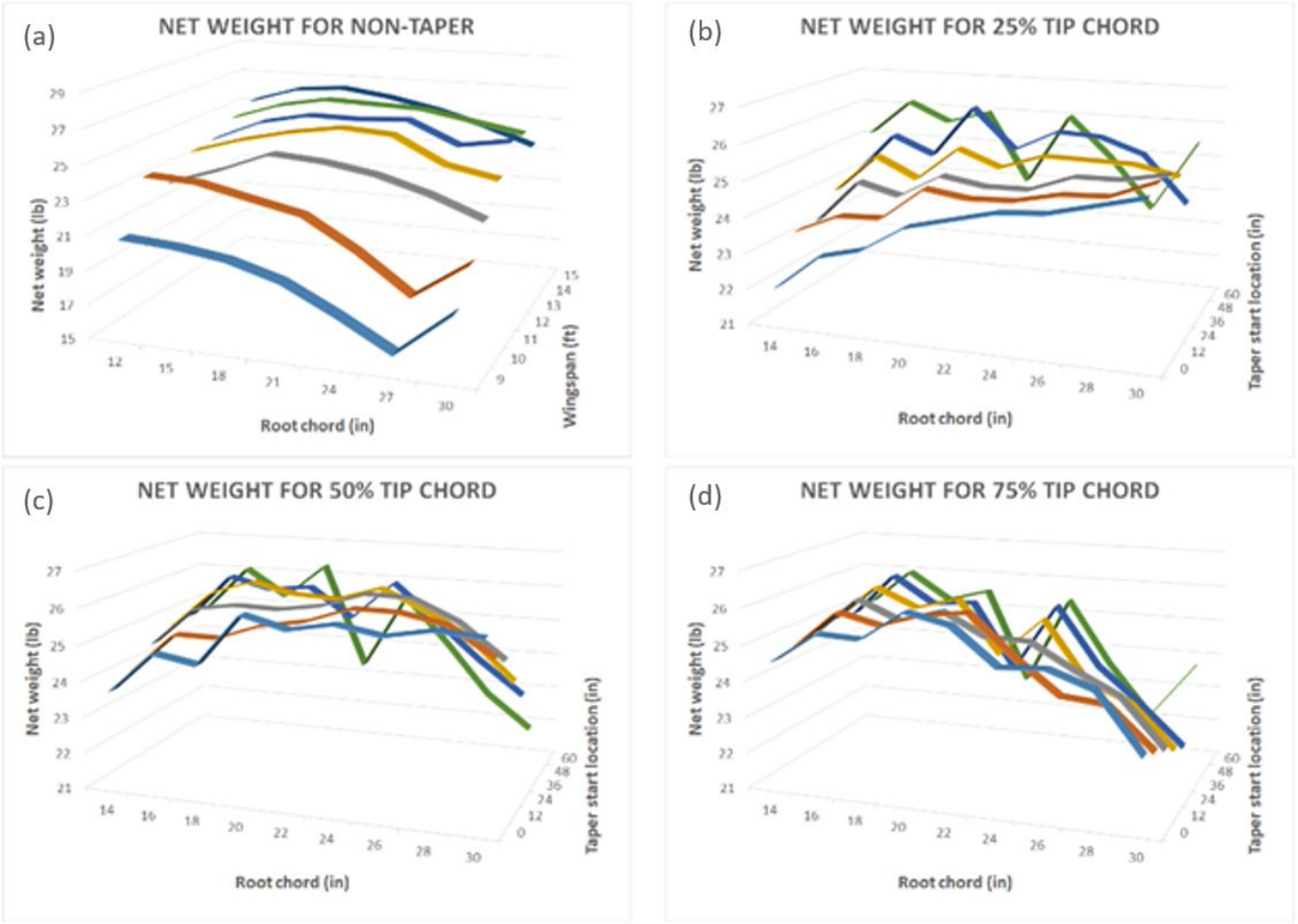

Figure 4.3.2: Net Weight for Different Variables

The four graphs all show a same pattern comparing the the allowable weight graphs: the net weight increases in the beginning and drops at the end as the wing reaches the 30 in root chord. This indicates that the wings with large root chord length have their weight increased more than the generated lift can compensate. As a result, the high net weight wings tend to have their root chord length between 18 and 24 in. This is one of the main factors used to determine the best wing design.

4.4 Final Wing Selection

Using the methodology presented in Sections 4.2 and 4.3, the wing shape shown in Figure 4.4.1 was selected for the final design. The wingspan is 12 feet with a 20 inch root chord and a 1 foot tapered section at the wingtips. The chord length at the wingtips is 10 inches. This wing was calculated to provide the highest net weight capacity. The simulated wing is able to lift 31.7 lbs at a takeoff distance of 200 feet. The fully constructed airplane was estimated to be 17.1 lbs and was finally weighed with a scale to be 17.3 lbs, leaving 14.4 lbs for passengers and luggage.

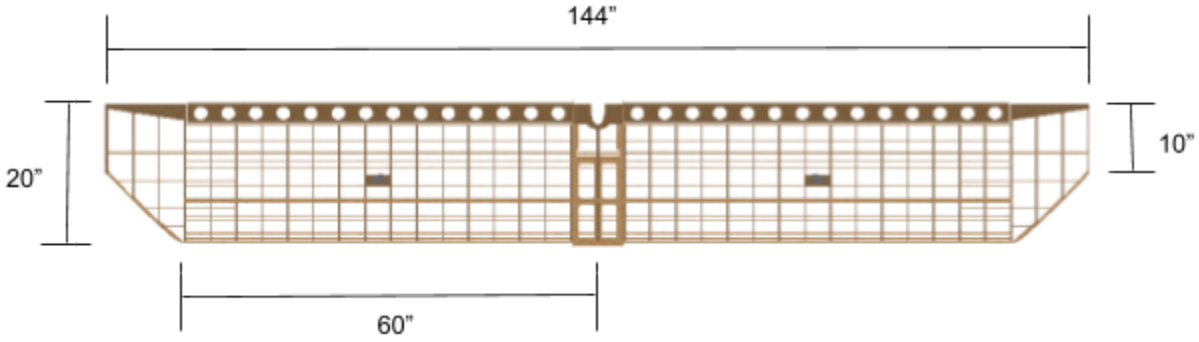

Figure 4.4.1: Final Wing Design

According to the per-round flight score equation (FS) in Figure 4.4.2, $100 is awarded per passenger and only $50 per pound of luggage. The score is maximized each round by carrying the most passengers since they are worth more per-unit than luggage. Therefore, the team calculated passengers carried using the minimum 0.5 lbs of luggage per passenger to allow for as many passengers as possible. Under these conditions the plane will be able to carry 22 passengers. This results in a per-round flight score of 2750 and a Final Flight Score of 68.75.

$$FFS = \ Final\ Flight\ Score = \frac{1}{40\ N}\left[\sum_{1}^{N} FS\right]$$

$$FS = Flight\ Score = \$100P + \$50C - \$100E$$

Figure 4.4.2: Scoring Equation

Test flights of the fully constructed plane verified the passenger and luggage calculations. The flights also revealed that the fully loaded airplane can take off in approximately 150 feet, significantly less than the 200 feet competition limit. The plane was not flown at full capacity, but test flights at 50% and 75% capacity had takeoff distances of roughly 50 feet and 100 feet respectively. Thus, the real-world takeoff distance for the fully loaded plane was estimated to be 150 feet. The difference between the calculated and actual takeoff distances is likely due to conservative values for factors such as wheel deflection, which contributes to drag during takeoff.

4.5 Stability

Longitudinal stability is dependent on the horizontal stabilizer. The effectiveness of the stabilizer is represented in the root locus graph obtained from CFD software, shown in Figure 4.5.1. Each point on the graph represents a longitudinal mode of oscillation. Points to the left of the imaginary axis reflect damped oscillations and points to the right reflect underdamped oscillations. All of the points on the longitudinal root locus graph for this plane indicate damped oscillations and stable flight. The real axis corresponds to a frequency of zero, and points further away from this axis have higher oscillatory frequencies.

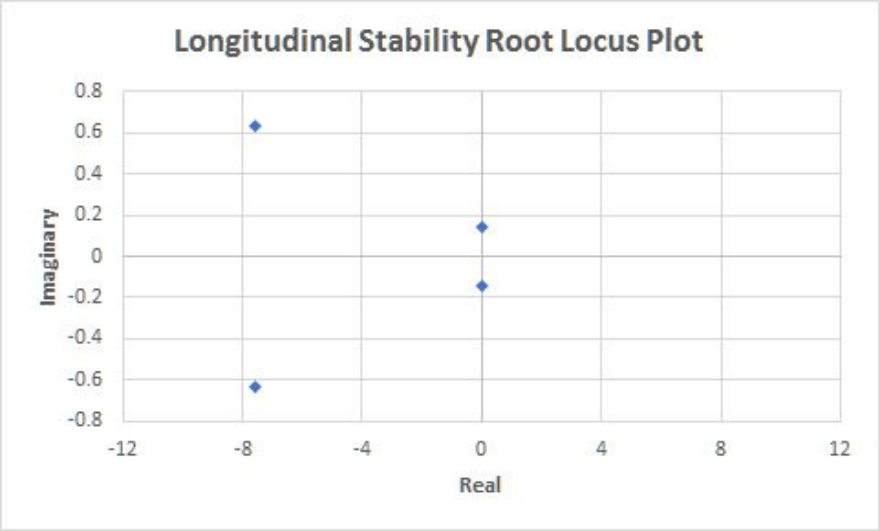

Figure 4.5.1: Longitudinal Root Locus Plot

The size and location of the horizontal stabilizer was adjusted iteratively to achieve damped oscillations with low frequencies while stabilizing the aircraft at zero angle of attack, where the wing achieves the highest lift to drag ratio. The horizontal stabilizer is placed 6 feet back from the leading edge of the wing. Specific dimensions are listed in Table 4.5.1 as well as in the engineering drawing of the final design in the appendix.

Table 4.5.1: Horizontal Stabilizer Dimensions

	Span (in)	**Chord Length (in)**	**Area (ft^2)**
Horizontal Stabilizer	69	12	5.75

Lateral stability was also measured according to a root locus graph, shown in Figure 4.5.2 below. Stability was achieved using a center of gravity positioned below the wing and a vertical stabilizer placed 6 feet back from the leading edge of the main wing.

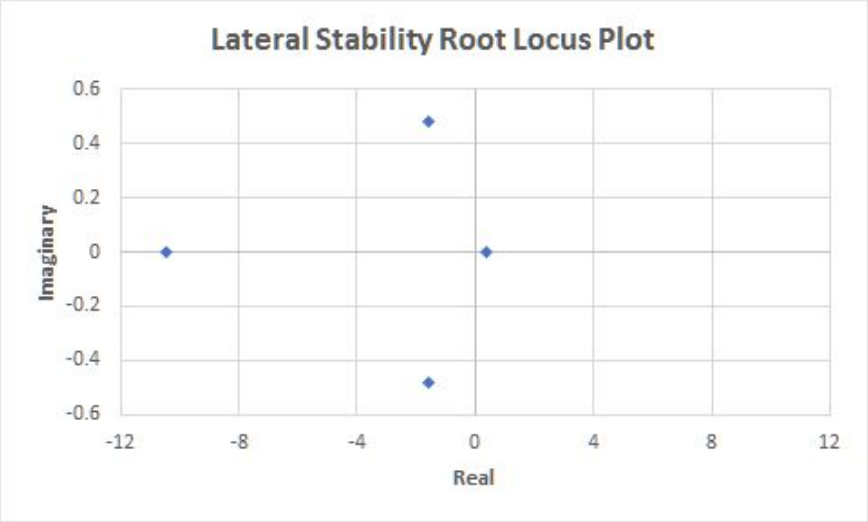

Figure 4.5.2: Lateral Stability Root Locus Plot

There is still one point to the right of the imaginary axis in the root locus graph, indicating one mode of instability. This is characterized by a tendency to very slowly continue in the direction of a yaw/horizontal disturbance. The team found that the only way to correct this was to incorporate a large amount of dihedral on the main wing but that would complicate manufacturing. Since a small yaw correction by the pilot would be sufficient to return the plane to normal flight, the team deemed the vertical stabilizer, low CG, and piloting ability sufficient for lateral stability. The dimensions for the vertical stabilizer are detailed in Table 4.5.2

Table 4.5.2: Vertical Stabilizer Dimensions

	Height (in)	**Chord Length (in)**	**Area (ft^2)**
Vertical Stabilizer	24.25	12.4	2.088

5.0 Structural Design

5.1 Wing

The wing in Figure 5.1.1 was designed with balsa and spruce. The winglets reduce drag and turbulence at the wing tips by preventing air from slipping off the tip of the wings and forming vortexes. Two major spars support the weight while smaller stringers help to support monokote attachment and add additional rigidity.

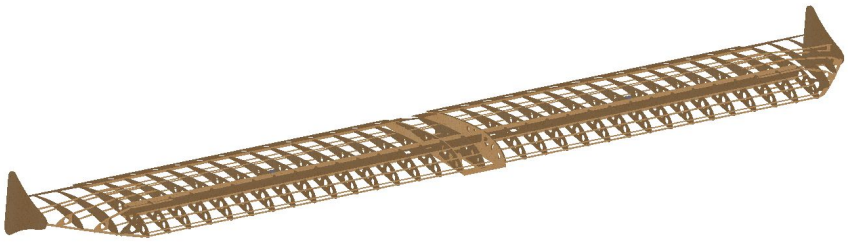

Figure 5.1.1: Wing Rendering

Table 5.1.1 lists all the major dimensions for the wing. The total area is roughly 20 ft^2 which gives a high amount of area for lift. Lastly, the aileron was sized to be about 12% total area of the wing for both sides. This is a common percentage when designing planes.

Table 5.1.1: Wing Dimensions

Length	143.5 inches	**Aileron Chord**	4 inches
Chord	20 inches	**Aileron Area**	2.33 ft^2
Area	19.93 ft^2	**Percent Area Aileron**	11.7%
Aileron Length (half)	56 inches		

Figure 5.1.2 shows a cross section of the wing to illustrate the final form of the S1223 airfoil. The main support spars are placed on the wing 6 inches back from the leading edge which is about where the center of lift of the plane is. An I-Beam configuration is made by adding a small balsa section to act as a web between the support spars. Lightening holes are used to reduce weight.

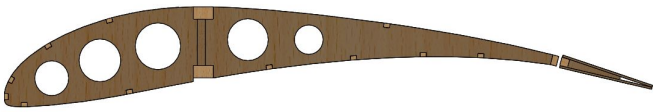

Figure 5.1.2: Wing Cross Section View

5.2 Fuselage

The fuselage and landing gear are shown in Figure 5.2.1. The battery and ballast box are placed 1.75 inches behind the propeller motor to ensure ideal center of gravity (CG) location.The propeller and motor are held by ¼” thick spruce.

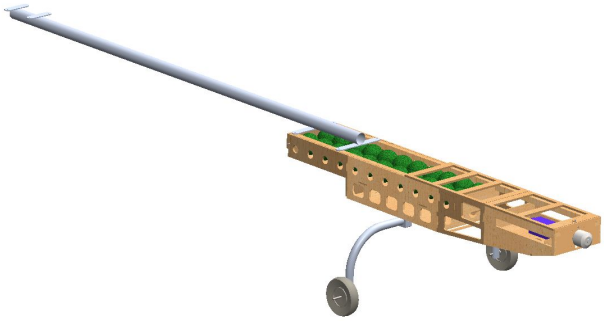

Figure 5.2.1: Fuselage Rendering

Table 5.2.1: Key Fuselage Dimensions

Length (motor plate to tail trailing edge)	9.26 ft
Wheel separation	24”
Angle at rest	8.5 degrees

The weights have a hole in the center and fit onto a threaded rod. Their location can be moved fore and aft with wing nuts to adjust the plane’s CG. The CG is between 5” and 6.5” from the leading edge. The weight box slides into the back of the fuselage box and is held in place with a bolt.

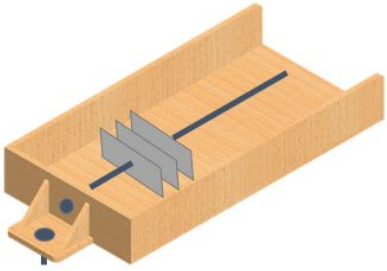

Figure 5.2.2: Slider Weight Box

The wing and tail section are connected with a 1.5” OD, 0.035” wall thickness aluminum tube. The tube has plates welded to create the attachment points for the fuselage box and tail section.

5.3 Tail

The tail assembly found in Figure 5.3.1 is comprised of spruce spars with balsa profiles.

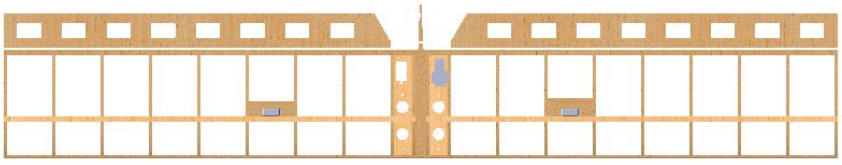

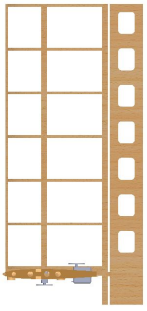

Fig 5.3.1 Tail Section Vertical and Horizontal Stabilizer

The elevator is split to accommodate the rudder. The base mounting plate is ½" spruce to connect to the fuselage. Servo mounts are placed between ribs. Rib spacing was chosen to be 4" to minimize monokote dimpling and contribute to the overall rigidity of the structure. Tail section profile for vertical and horizontal stabilizers was chosen to be NACA 0008 due to its symmetric airfoil and minimal drag characteristics during flight. The vertical stabilizer spars fit into slots on the horizontal stabilizer. To further increase rigidity between the horizontal and vertical stabilizers, bracing wires are installed.

The elevator was divided to allow for the extension of the rudder below the horizontal by 3.25". The tailwheel is then controlled by the rudder action through a spring a pivot system. Other possibilities for tailwheel control involved inserting a control rod into the rudder itself. The spring and pivot tailwheel control system was chosen to reduce the amount of hard attachment to the rudder in case of tailwheel support failure. In the case of such a failure, the aircraft rudder would still be operational.

Table 5.3.1: Wing and Tail Dimensions

Horizontal Length	69 inches	**Vertical & Rudder Area**	2.11 ft^2
Horizontal & Elevator Chord	12 inches	**Vertical & Rudder Chord**	12.4"
Elevator Length (Half)	32 inches	**Rudder Area**	0.76 ft^2
Elevator Chord	4 inches	**Vertical length**	24.25"
Percent Area Elevator	30.7 %	**Rudder length**	27.5"
Horizontal and Elevator Area	5.75 ft^2	**Rudder Chord**	4"
Elevator Area	1.77 ft^2	**Percent Area Rudder**	36.0%

A standard rule of thumb for control surface sizing was applied by using an approximate 25% of stabilizer to control surface area; the elevator was found to be 0.89 ft^2 while the rudder required 0.76ft^2. Control surfaces are mounted using heavy duty cotter pin hinges mounted within the trailing edge of the stabilizer and leading edge of the control surface. Using cotter pin hinges contribute to the rigidity of the control surface while reducing the amount of energy need to turn the hinge itself.

5.4 Landing Gear

The main landing gear was made from bent aluminum tubing with an outer diameter of 1.5” and wall thickness of 0.035” . The tail wheel was purchased, and is made steerable by attachment to the rudder. The landing gear type is conventional, with a tail wheel that lifts off the ground once the plane reaches a certain velocity. The distance between the wheels is 24 inches for stability. Figure 5.4.2 shows the acceptable angles for a taildragger (8). These angles were placed in SolidWorks with given dimensions from the plane to determine wheel placement. The landing gear lifts the bottom of the fuselage 1 ft from the ground. The landing gear is placed 6 inches in front of the CG as an optimal distance for balance during takeoff (8). The wheels are high density foam with a rubber skin. In previous planes, soft, low density foam wheels were used, which had large deflection and added significant drag. This year’s wheels are rated for 50 lb planes for minimal drag.

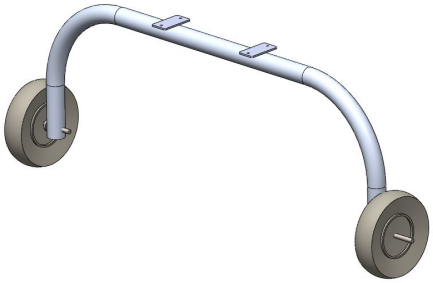

Figure 5.4.1: Landing Gear

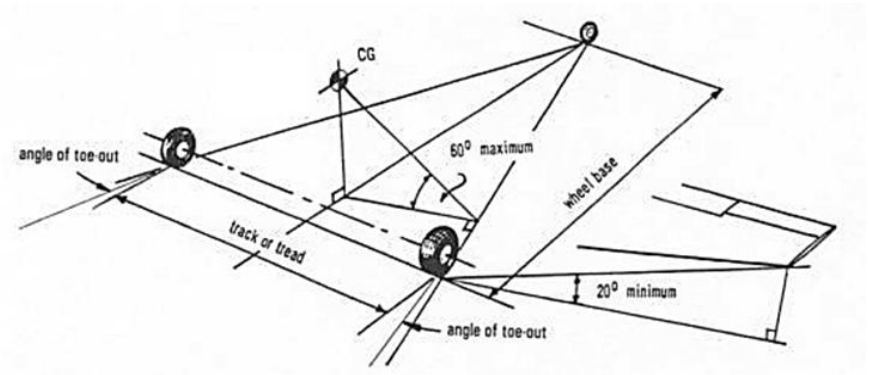

Figure 5.4.2 Landing Gear Placement (8)

5.5 Connections

The connections between the tail section, wing, landing gear, and fuselage are shown in Fig 5.6.1. The main connecting structure is the aluminum tube with welded plates. The tube mounts on top of the fuselage with, and the wing mounts over the tube onto the fuselage, both with bolted connections. The tail section bolts onto a welded plate on top of the tube. The landing gear bolts to the bottom of the fuselage, underneath the weight compartment. The tail wheel mounts to the bottom of the tube. All of the bolts connecting to the aluminum tube are #6-32.

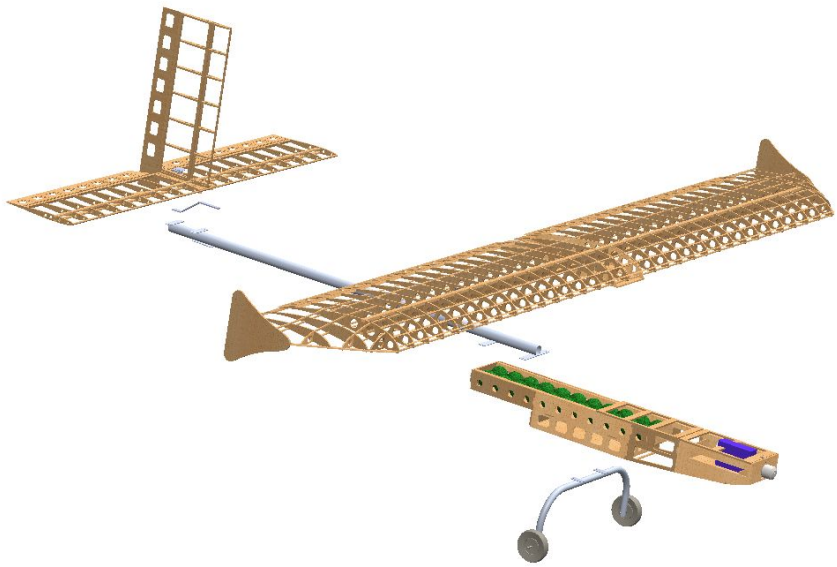

Figure 5.5.1: Exploded view

6.0 Manufacturing and Material Selection

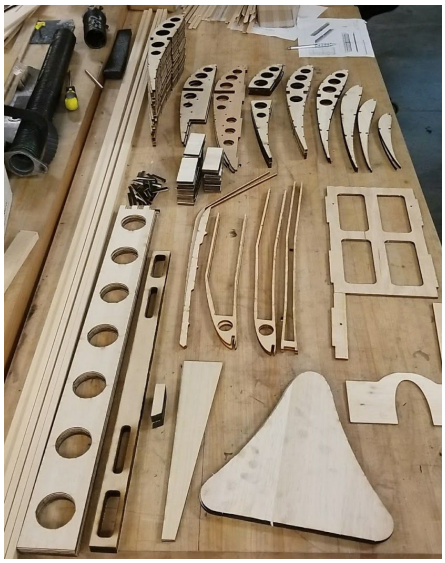

Figure 6.0.1: Cut-out Parts

The wing, tail and fuselage were all modified for ease of repairing parts. The wing and tail foils are made of balsa since the spruce spars hold the bending loads of the wing. These sections are laser cut for accuracy and then sanded and edge cleaned with alcohol before covering. CA adhesive was used to tack the parts together, then epoxy glue was applied to strengthen the connection. Notches are used for alignment. The tail section is made in two parts : horizontal, and vertical stabilizers made of balsa foils with spruce

spars for the bending load during flight.

The fuselage uses two main spruce beams to hold the loads of carrying the weight of both passengers and luggage. Those two beams lead into an aluminum tube since the length of the plane requires a higher yield strength from the torsional and bending during flight with possibly rough conditions. This could have been accomplished with thicker spruce beams or denser wood, but the ratio of strength to weight would be too high.

Balsa was chosen for the non-structural components because of its extremely low density and sufficient strength. Spruce was chosen for its high strength to weight ratio and availability in specialized dimensions.

Table 6.0.1: Wood Comparison

Type of wood	**Balsa**	**Spruce**	**Pine**
Max shear strength (psi)	1000	1,230	1170
Density (lb/ft^3)	10	28	22
Strength to Weight Ratio (Shear strength/Density)	100	43.9	53.2

7.0 Electronics

7.1 Motor and Propeller

This year, analysis was done with a lower KV motor and a higher diameter prop because higher diameter propellers are more efficient (9). The motor selected was a 260KV motor. Specifically, a Turnigy SK3-6354 260KV motor was chosen. Figure 7.1.1 explains how the propeller was chosen given this motor choice. Figure 7.1.1 shows how the effective thrust changes with velocity using a dynamic equation for thrust. The highest watt pull is expected at static thrust. Each line represents a different propeller diameter with a calculated pitch that would give 1000 Watts for static thrust.

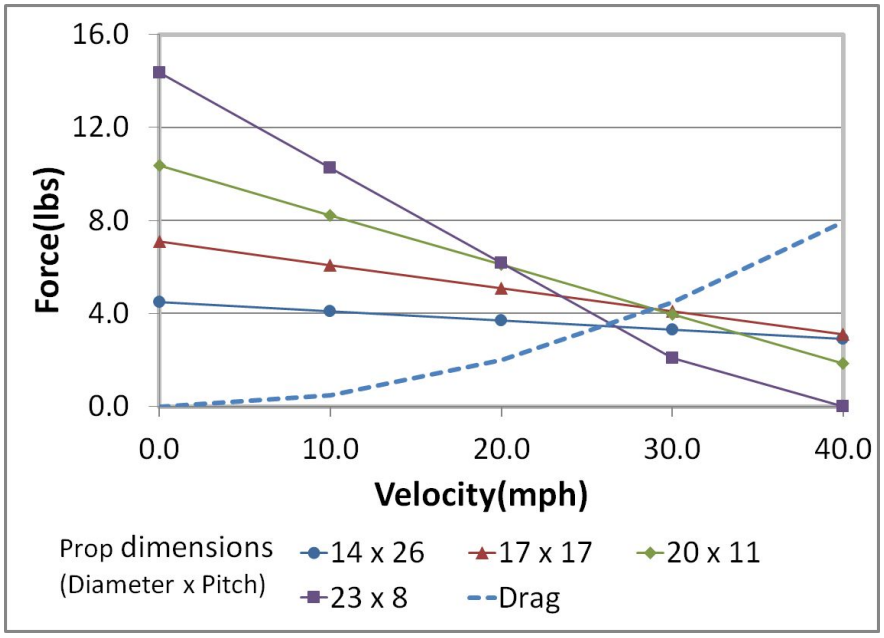

Figure 7.1.1: Graph of Force for Velocity Given a Propeller with a 260KV Motor

The analysis in Figure 7.1.1 illustrates the performance of various motor and propeller combinations. A high diameter - low pitch propeller such as the 23 x 8 would give high initial thrust during takeoff but has lower thrust during flight. Alternatively, a high pitch - low diameter propeller would give low thrust at takeoff but higher thrust at high velocities. The maximum velocity can be determined by the intersection of the drag curve and the thrust curve. The intersection with the highest velocity is the propeller chosen to further analyze. For Figure 7.1.1 it appears the 17" x 17" prop and the 20" x 11" prop are the best and have about the same intersection. However, since they are the same, the 20" x 11" has a higher initial thrust, which can improve takeoff. Therefore the 20" x 11" was picked as a start for a propeller to test with for a 260KV motor.

The next step would be to order the most equivalent props available in the 20" x 11" size and run static prop tests. Different types and different manufacturers were selected to test props this year including Graupner or APC propellers and wide or electric propellers. The manufacturer type did not seem to have much effect on results and predictions. However, wide style propellers varied significantly from electric propellers. A percent error calculation was made by comparing the static thrust prediction from Figure 7.1.1 to the actual test results in Figure 7.1.2. The wide propellers are much thicker and

heavier and based on predictions it gave a 32% error. All electric propellers were within 12% error. Last years propellers were also compared. Figure 7.1.2 and 7.1.3 show how the static tests were run and the results. In Figure 7.1.3 a right angle wood assembly is hinged so the force of the propeller can act and be read by the scale. Figure 7.1.3 pictures the motor tests done with both low KV - high diameter propellers and lower diameter propeller - higher KV motors.

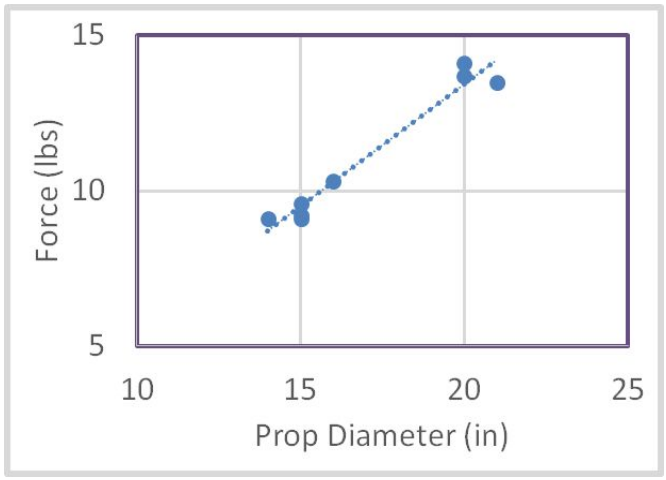

Figure 7.1.2: Prop Diameter Versus Force Test Results

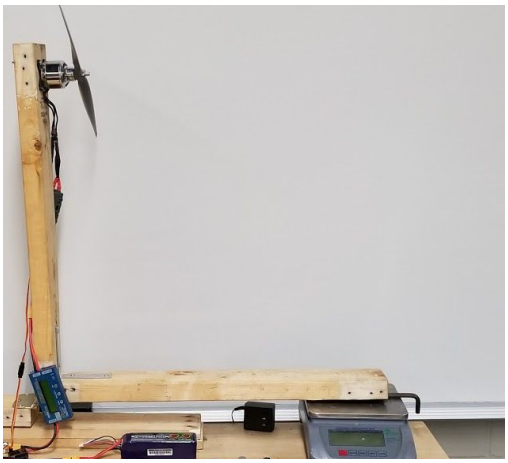

Figure 7.1.3: Test Stand Setup

Figure 7.1.2 helps to illustrate the improved effect larger propeller lower KV motor systems have. For static thrust there is a 40% increase in thrust. This helps to verify the assumption at the beginning of this section that these systems are more efficient. Therefore, a larger prop with a lower KV motor was placed on the plane this year. Specifically, a Graupner 20” x 10” E propeller was chosen. While the APC wide propeller gave slightly better results, the Graupner electric propeller was chosen over the APC prop because it was both lighter and had a very noticeable decrease in vibrations. The vibration was evaluated by sound and test stand motion during the test.

7.2 Electrical Systems

Once the propeller and motor are chosen the rest of the components are chosen. These components are all listed in Table 7.1.1. The maximum current at 22V for 1000 watts is expected around 45 Amps. Therefore the Talon 90 Amp ESC and the XT60 connectors which can handle up to 60 amps are both rated appropriately for these requirements. Since a long length of wire is required for the arming plug, thicker 10 awg wire was chosen to help reduce power loss. The battery, at 3300mAh, was

determined conservatively to have a flight time of about 5 minutes which is plenty for one round of flight. This was determined by dividing the max current pulled of 45 amps by the 3.3 amp hours of the battery and multiplying by 60 minutes per hour.

Table 7.2.1 Electronics

ESC	Talon 90A ESC
Battery	Turnigy Nano-tech 3300mAh, 6S, 25-50C
Wire	10 awg
Connectors	XT60
Propeller	Graupner 20x10E
Motor	Turnigy SK3-6354 260KV

8.0 Loading and Environmental Assumptions

The loading applied in Sections 9 and 10 comes from three main sources: lift from the wing,weight of the stabilizers, and forces generated by deflecting the tail control surfaces. Control surface loads were calculated by modeling the surfaces as flat plates that receive the dynamic pressure created by the air's relative velocity as the plane flies. The surfaces were assumed to be fully deflected at 40 degrees to capture the maximum force acting on each surface, perpendicular to and at the center of each surface.

Impact force on the landing gear was calculated by determining vertical acceleration during landing and multiplying by the mass of the airplane. Conservative values for a descent rate on landing and impact time were 4.5 mph and 0.1 seconds respectively. These were used to compute impact acceleration, and finally an impact force. Table 8.0.1 details all forces considered in Section 9 and 10 and their sources.

Table 8.0.1: Critical Loads and Sources

Source	**Force (lbs)**
Wing Lift	31.70
Elevator	2.86
Rudder	1.19
Aileron	1.82
Tail Section Weight	1.3
Landing Impact	100

9.0 Structural Analysis:

9.1 Wing

When analyzing wing strength, bending was considered the most critical load, so the equation bending stress = MC/I was used. Four main wing structures were considered to add bending strength: Circular Spar, Rectangular Spar, C-Channel, and Parallel Split Spar, as shown in Figure 9.1.1.

Figure 9.1.1: Proposed Spar Configurations

For weight comparison purposes, each shape was analyzed as if it had a 1 in^2 of material, and the maximum bending stress was calculated using $\sigma = MC/I$. The moment used was derived from the fluid analysis. The distributed load on the wing during flight is calculated to be 0.01134 psi. To be conservative, the wing load is applied as a point load at the ends of the wing. This results in a 15.65 lb force at 6 ft, giving a moment of 1127 in-lbs. The results are tabulated below in Table 9.1.1.

Table 9.1.1: Spar Shape Comparison

Shape	**Inertia (in^4)**	**Maximum Experienced Bending Stress (psi)**
Square cross Section	.083	6763
Circular Cross Section	.080	2995
Channel	1.036	1631
Parallel Spars	1.864	580

The parallel spars experienced the lowest bending stress, so this design was chosen. Thus, the spars used were sized ⅜ in by ⅝ in, giving a final factor of safety of 4.51. This gives a maximum deflection of 2.27” under normal flight loads. Additional stringers are added for stiffness, torsion resistance, and monokote attachment. More detail is shown in Appendix 10.

9.2 Tail

For the tail section, similar logic was utilized to select the support structure design. The distributed load on the tail is 0.00831 psi. To be conservative, the moment is assumed to be the entire distributed load applied at the ends of the tail. This results in a 1.65 lbf at 3ft (36 in), giving a moment of 59.4 in-lbs. The parallel spar design is also used in the tail section, with sizes ½" by ¼". Like the wing, additional stringers are added for extra support. To minimize deflection, the spars are oversized, giving a deflection of 0.01" with a FS of 5.22.

9.3 Tube

Various boom designs were considered for this plane. Wood and aluminum were considered. However, tests in appendix A8 revealed that wood experienced large deflections when flight loads were applied. Then, aluminum was considered. For torsional stiffness and strength, a circular tube is the optimum shape.

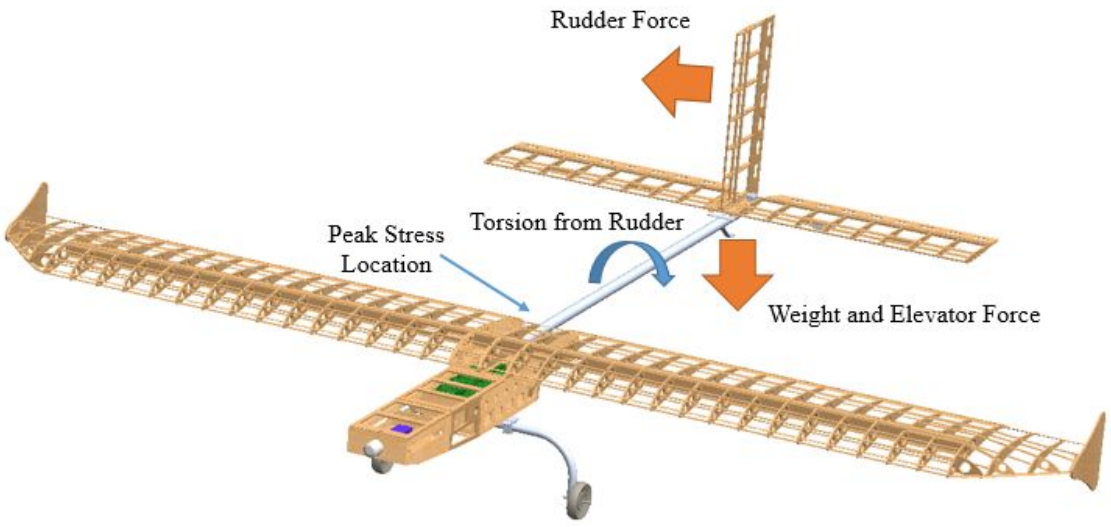

Figure 9.3.1: Tube Load Application

There is significant dynamic load between the wing and the tail. Torsion from rudder movement, bending from aircraft weight,bending from rudder movement, and bending from elevator movement all apply. Fluid analysis provides loads shown below. Each load is modeled as a worst case scenario with loads described in Section 8.

Table 9.3.1 Tube Stresses

Type	Cause	Moment (in lbs)	Stress Induced (psi)
Bending	Elevator	140.4	2918
Bending	Weight	108.0	2245
Bending	Rudder	58.5	1216
Torsion	Rudder	12.6	131

VM Equivalent Stress	3880	psi
Yield Strength of 6061 Aluminum	40000	psi
Factor of Safety	10.3	

Deflection was also calculated, and different size tubes were simulated to reduce the deflection to 1.08 in and 1.4 degrees. A smaller size could have been chosen to reduce FS and weight without yielding. However, this would have had a large deflection which would hurt plane performance.

9.4 Landing Gear

The landing gear was analyzed using a load derived from the impact created by a hard landing, 100 lbs. To be conservative, this load was applied to one side of the landing gear, assuming uneven landing. To size the landing gear tube, both shear and bending stresses were considered. The Von Mises equivalent stress was considered for the factor of safety. The landing gear was modeled as a cantilever beam with a 50 lb load applied at the wheel distance, 12 inches from center. The final size is 1” outer diameter with a .095” wall thickness.

Table 9.4.1 Landing Gear Stresses

Shear Stress on Cross Section	185.2	psi
Bending Stress at Center	21473	psi
Von Mesis Equivalent	21473	psi
6061-T6 Aluminum Yield Strength	30000	psi
Factor of Safety	1.40	

10.0 Servo Sizing

Servos were sized based on the control surface loads calculated in Section 8 and the linkage geometry connecting the servos to the control surfaces. All control surfaces are actuated by a rigid control rod connected directly to a servo. The highest torque that a servo must deliver to a control surface occurs at that surface’s maximum deflection, 40 degrees. Tracing a control surface load through the control linkage yields the torque a given servo needs to deliver. Servos rated at 188 oz-in were found

to be suitable for all control surfaces. One servo is used to control each control surface, except the elevator. Since the elevator is split in half to allow for rudder movement, one servo is used to control each side of the elevator and only needs to deliver half the torque necessary for the entire surface. Table 10.0.1 details the torque each servo needs to deliver and the factor of safety for each. The factor of safety is the necessary torque needed at maximum control surface deflection compared to the rated torque for each servo.

Table 10.0.1: Necessary Servo Torques for Control Surfaces

Control Surface	Necessary Torque (in-lbs)	Factor of Safety
Elevator (one half)	7.05	1.67
Rudder	5.88	2.00
Aileron	10.38	1.14

11.0 Conclusions

The final design was completed within the parameters set by the SAE Aero Design Challenge. This year's plane is a mono-wing plane with a 12 foot wingspan and backward sweep. The projected flight score per round is 68.7 carrying 22 balls and 11 pounds of luggage, which was verified by testing. At the competition, the Regular Class Team placed 2nd in the Oral Presentation segment out of 37 teams, including international teams. The first place team was from Poland, making TU the highest scoring American team in oral presentations. TU also received 4th in the written reports. Unfortunately, there were no completed flights at competition. During the first flight, the plane took off easily, but experienced a slow descent and crash. Post-mortem analysis revealed a malfunctioning servo and issues connecting to the receiver. These were thought to be the cause of the crash. The plane was rebuilt with spare parts and flew again in the fourth flight round. The plane slowly descended and and crashed again. After this flight, a range test was performed with the transmitter. These revealed range issues with the transmitter, which is assumed to have caused all three crashes. The plane itself did not cause the crash, and the engineering work was valid. The problem was with the transmitter, a purchased component that

had not previously caused issues. Despite a zero flight score, the team placed 9th in the Regular Class overall.

12.0 Table of Referenced Documents, References, and Specifications

#	Source	Use
1	http://m-selig.ae.illinois.edu/ads/coord_database.html	Airfoil Data Points
2	Cengel and Cimbala, Essentials of Fluid Mechanics: Fundamentals and Applications	Lift and Drag Calculations
3	https://www.grc.nasa.gov/www/k-12/airplane/lifteq.html	Lift and Drag Calculations
4	Aircraft Structures: David J Peery	Structural Design and Analysis
5	Airframe Stress Analysis and Sizing: Niu	Structural Design and Analysis
6	https://www.faa.gov/uas/getting_started/	Federal Aviation Administration Standards
7	Propeller Static & Dynamic Thrust Calculation: Gabriel Staples	Thrust Analysis
8	Aircraft Landing Gear Layouts: Scott, Jeffrey A.	Landing gear placement
9	Propeller Efficiency, Rule of Thumb: David F. Rogers	Propeller Analysis and selection

13.0 Recommendations

- Do a lot of systems checks
    - Do a range test
        - A range test is a low power signal to see if you have good connection over a specific short distance
        - It may have caused all 3 2018 crashes
        - It is a mode on the transmitter. Read the manual for how to conduct a test.
    - Do a control surface check
        - Check that they can handle some load and if they move enough.
    - Do an endurance test
        - Run the thing up for several minutes and see if everything still works.
- Try to be innovative
    - Our planes work really well, but TU always struggles with how to distinguish their design

    - For reports and presentation, there is a score for innovation and uniqueness. Try to come up with new design and manufacturing ideas.
- Build at least two of everything
    - Things break at competition. Without extra parts, there isn't anything the team can do.
- Start early
    - Finish CFD Analysis and Airframe design by mid-November.
- Design parts around what you can get from Lowes except balsa
    - Spruce was sized based on availability from Aircraftspruce.com
    - The spruce supplier ran out of wood in 2018 and the sizes weren't available from other vendors within the time limit
    - If the plane was designed around Lowes availability, it would have been easier to obtain materials for the rebuild.
- Use S1223 airfoil
    - When tests are always run, this one is always the best.
    - Copy results from before that show it is the best and just use it, don't waste your time.
- Avoid wing warp
    - It creates large difference in lift between left and right side requiring lots of aileron movement.
    - It is very evident in version 1 of 2018 plane.
    - This can be fixed by a foam form of wing underneath during gluing.
        - The foam form is made with a hotwire using templates cut with the plasma cutter.
    - There is an additional way to help fix this by putting tubes through foils during gluing
        - Lightening holes were set to exact OD used by sch-40 pvc pipe and foils were slid on.
        - This helps keep it straight and foils in line.

- Add “Stringers” for monokoting
    - A “Stringer” is a small piece of wood run on the surface of the foils and perpendicular to them. The 2018 plane had 3/16” by ⅛” spruce stringers set into the airfoils which had slots set for them.
    - Especially with the s1223 airfoil, this form is very difficult to come out well on the undercamber. Stringers help provide a surface when the foil is not enough for attachment.
    - The problem is evident on the 2017 underside wing, and part of the leading edge, but the leading edge was fixed other ways.
    - It is suggested to try 1/32” balsa in longer width for stringers (could also save design time and maybe mount on top, but play with this first).
- Add balsa sheeting on leading edge
    - This is a wood sheeting on the leading edge before the monokote is applied. 2018 used 1/32” balsa to sheet the front edge.
    - This problem is evident in the 2017 planes leading edge, there is quite a large amount of monokote pulling into itself.
- Make sturdy control surfaces
    - The 2018 design utilized spar with ribs and 1/16” balsa sheeting over top, size of spar determined by profile of foil.
    - This was much stronger than previous designs.
- Use ribs and spar design for horizontal stabilizer
    - The cross section of the tail isn’t super important to the flight characteristics.
    - A flat plate was considered instead of a ribs and spar design.
    - The plate would have to be heavy to be strong enough, so ribs and spar design is more efficient.

- Use two spars on edges instead of one big through center to reduce weight (See Structural Analysis Comparison)
    - It is especially useful in the wing but also evident in the vertical and horizontal stabilizer
    - This reduces weight because you can get a high inertia with spars mounted as far apart as possible.
    - 2016 used a large aluminum tube in the wing and was heavy because of this, avoid aluminum as much as possible, except in the case of landing gear and perhaps fuselage to the tail (by itself with a very large diameter and thin wall to reduce weight)
- Tube from fuselage to tail
    - The 2018 plane used a large tube 1.5” OD with very thin walls 0.032” to reduce weight. while aluminum is typically discouraged, this is a rare exception.
    - Both the 2017 design and early tests in 2018 showed massive torsional deflection in the fuselage for the tail. this is not acceptable. 2017 was fixed with a lot of extra wood and 2018 was fixed by switching to aluminum tube.
    - Normally a wood box is used to fix this but these can be heavy, so a tube was chosen.
- Avoid aluminum expect in specific cases
    - Don’t make a aluminum fuselage. The 2016 team made one and it was terribly heavy.
    - Aluminum fuselage can also cause signal interference.
    - Aluminium fuselage is difficult to modify if needed.
- Consider wiring when designing the fuselage
    - Wiring was forgotten in 2016. This is especially hard to modify considering the fusealge in 2016 was also aluminum.
- If using aluminum, bolt it or add gussets
    - Try to avoid welding if possible.

    - A aluminum tube makes a good landing gear, but plates might be needed to mount it. welding aluminum is spotty at best
    - 2018 plane had a tube welded to plate, which broke off while rolling it to the runway. It was repaired by drilling through the plates and adding bolts in time to make the flight round.
    - Large thin wall tube use for the fuselage to tail connection is tricky to work with. Welding may be necessary if bolts will bend tube. Gussets should help.
- Use lock nuts on bolts for wheels
    - A wheel fell off during 2016 takeoff because the wheel pushed up against the nut and spun it off
- Use servo wire clips
    - They keep servo connections from coming unplugged when using servo wire extenders
- Hinge slot for control surfaces
    - This is done with the slotting tool (oscillating tool) , its a long, thin cut. it cuts into the middle of the thin wood on the plane side and then the middle of the spar on the control surface side. then hinges are fit into both with glue.
    - It comes out way better, it holds in place better and makes for a better, safer plane.
    - Added in 2018, not there before.
- Have tail wheel steering, control it by the rudder
    - Using springs the tail wheel can attach to the sides of the rudder and move when it moves. These devices are easy and commercially available.
    - It is easy and they are commercially available.
- Store batteries at storage charge
    - There's a setting on the charger for this

    - If left fully charged for a year they swell and go bad and could be dangerous and cause a LiPo fire if used.
    - Furthermore, be careful with LiPo they are very dangerous.
- Use tee nuts
    - Tee nuts dig into wood and stay there when bolt is removed
    - Tee nuts can hold bolts for modular components and don't have to be removed which is useful if access is restricted or covered in monokote.
    - Tee nuts are great for components you want to easily unbolt and re-bolt
- Don't waste your time with TU's wind tunnel
    - Scaling laws mean TU's wind tunnel cannot reach speeds necessary for a properly scaled test.
    - Tipton may have a contact with a Boeing facility in st Louis if you still want to.
- Do a hard point analysis
    - This is the analysis for the joints between then main members including the fasteners and their locations.
    - It is important for analysis to determine these points will not break apart. These are a very likely place to break apart.
- Check the presentation and inspection schedule
    - It is posted a week or so before competition on the SAE Website.
- Be ready to register for the competition immediately when it opens
    - It sells out within 40 seconds!
    - If this is missed the team will be put on the waitlist and may not be able to go to competition.

Appendix:

A1: Acknowledgments:

The success of this year's SAE Aero Senior Project goes beyond the scope of capabilities of any team. An outstanding array of sources and dedicated individuals made the team and we are especially grateful for the plethora of time they spent. The following represents the incredible people and considerate organizations that made this year possible:

- TU Mechanical Engineering Department for Funding and Support
- Luann Moon for being a godsend and persuading vendors into cooperation
- Terry and John at North Campus for manufacturing assistance
- Dean Sorem for being the Team Advisor and providing guidance
- KC BluePrint for printing scale models
- Mike Pennell with Glue Dobbers for flying lending components
- Mark and Bart Shelts for help building shipping containers and providing the trailer to transport crates to Gunnebo Johnson
- Gunnebo Johnson for offering their shipping services at a discounted rate
- Triumph Aerostructures for donating packing materials
- Friends willing to review the SAE Design Report before submission
- Jamie for helping to drive to the field for a test flight and picking up the plane from gunnebo.

A2: List of Symbols and Acronyms

2D	Two dimensional	V(v)	Velocity
3D	Three dimensional	v	Initial velocity
A	Area	V	Max Velocity
a	Acceleration	W	Weight
C_D	Drag coefficient	X	Final distance
CFD	Computational Fluid Dynamics	x	Initial distance
C_L	Lift coefficient	μ	Dynamic viscosity
D(v)	Drag	TU	University of Tulsa
f(v)	Friction between the airplane and runway	kV	rpm/Volt
L	Lift	rpm	Revolutions per Minute
NACA	National Advisory Committee for Aeronautics	mAh	milliamp hours

T(v)	Dynamic Thrust Generated by Propeller	ESC	Electronic Speed Controller
$T_{net}(v)$	Net Thrust	ρ	Density
t	Time	p_0	Air pressure at sea level

A3: Payload Prediction Curve Density Altitude

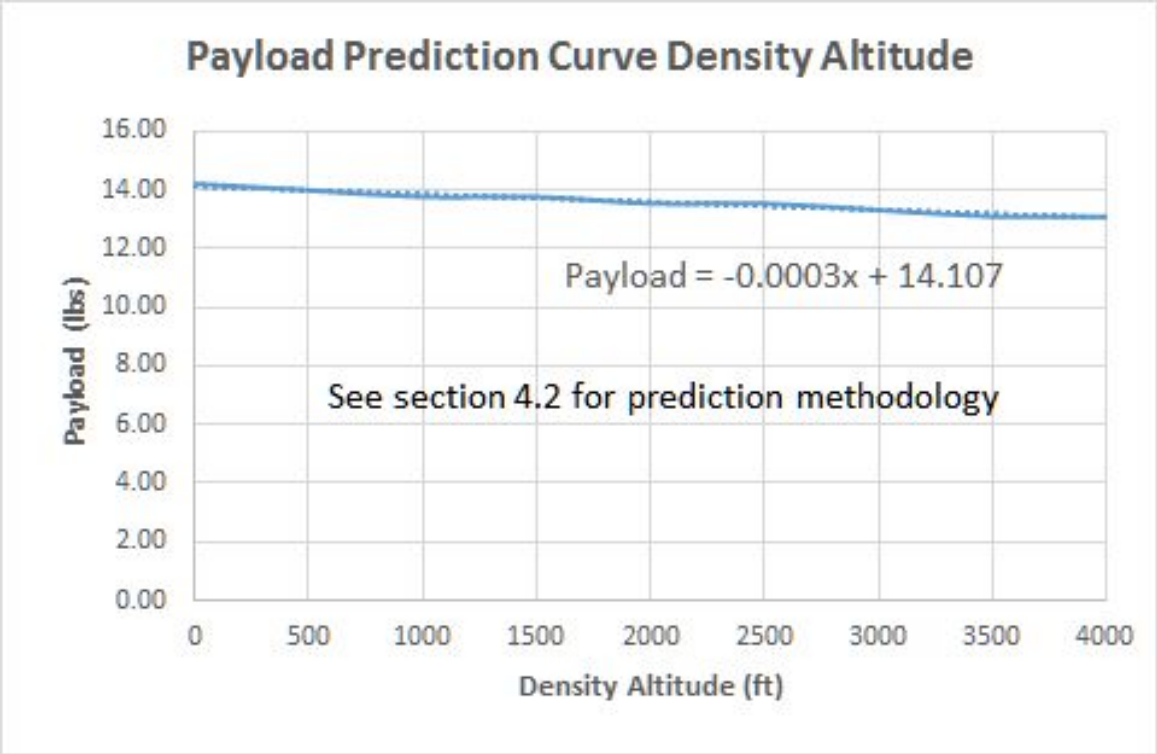

A4: 2D Drawings

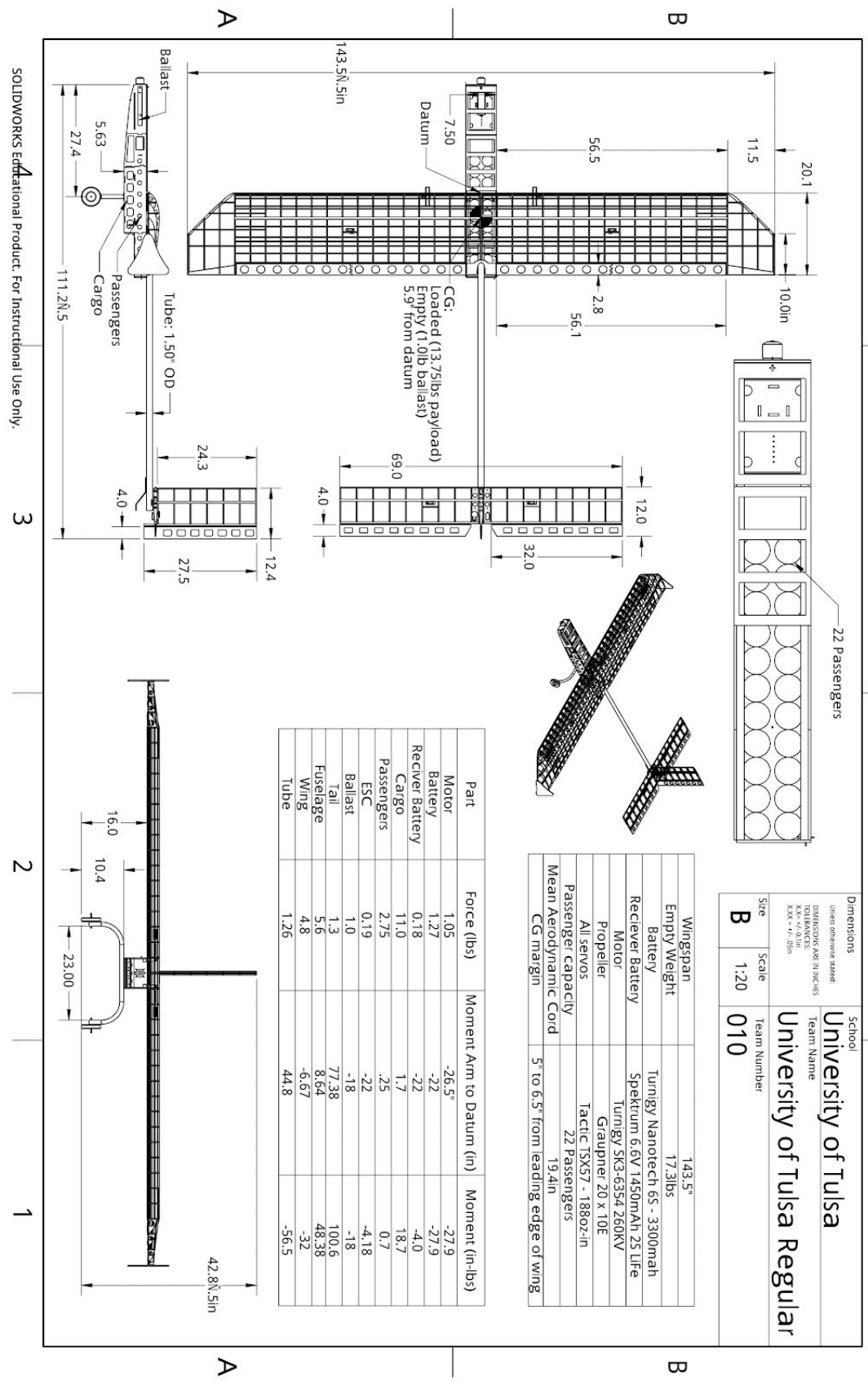

Wingspan	143.5"
Empty Weight	17.3lbs
Battery	Turnigy Nanotech 6S - 3300mah
Reciever Battery	Spektrum 6.6V 1450mAh 2S LiFe
Motor	Turnigy SK3-6354 260KV
Propeller	Graupner 20 x 10E
All servos	Tactic TSX57 - 188oz-in
Passenger capacity	22 Passengers
Mean Aerodynamic Cord	19.4in
CG margin	5" to 6.5" from leading edge of wing

Part	Force (lbs)	Moment Arm to Datum (in)	Moment (in-lbs)
Motor	1.05	-26.5"	-27.9
Battery	1.27	-22	-27.9
Reciver Battery	0.18	-22	-4.0
Cargo	11.0	1.7	18.7
Passengers	2.75	.25	0.7
ESC	0.19	-22	-4.18
Ballast	1.0	-18	-18
Tail	1.3	77.38	100.6
Fuselage	5.6	8.64	48.38
Wing	4.8	-6.67	-32
Tube	1.26	44.8	-56.5

ITEM NO.	PART NUMBER	Description	Stock material	Final dimensions (if applicable)	manufacturing	QTY.	Done
1	joiner	Center join wing together	Sheet: 5/8" spruce		Laser	1	
2	main spar	main spar	Strip Spruce	3/8" x 5/8" x 60.25"	Table Saw/chop saw	4	
3	trailing edge piece	tailing edge for taper	Sheet: 1/8" Balsa		Laser	2	
4	stringer	stringers	strip spruce	1/8" x 3/16" x 60.25"	Table saw/hack saw	22	
6	airfoil taper 1	closet to center taper airfoil	Sheet: 1/4" balsa		Laser	2	
7	airfoil taper 3	end taper airfoil	Sheet: 1/4" balsa		Laser	2	
8	airfoil taper 2	middle taper airfoil	Sheet: 1/4" balsa		Laser	2	
9	airfoil aileron	primary airfoil in front of aileron	Sheet: 1/4" balsa		Laser	22	
10	trailing edge center piece	center trailing edge pice curved over tube	Sheet: 1/8" balsa		Laser	1	
11	airfoil center1	centered airfoil	Sheet: 1/4" balsa		Laser	2	
12	aileron attach	spar at trailing edge wing for aileron hinges to attach to	stick spruce	1/4 x .304" x 56.25"	Table saw/hack saw	2	
13	mate plate	bottom plate to screw on fuselage	Sheet: .205" ply		Laser	1	
14	airfoil linkage	side plate to attach to mate plate	Sheet: 3/16" spruce		Laser	2	
15	aileron main foil	small triangle pices to support sheeting on aileron	Sheet: 1/4" balsa		Laser	34	
16	aileron cover	sheeting over aileron	Sheet: 1/16" balsa - (cut sheeting with tail pieces - only way it will fit - ask before)		Laser (ask before cutting)	8	
17	aileron spar	aileron spar to attach hinges too	sitck spruce	1/4 x1/4 x 56.05"	Table saw/ hack saw	2	
18	end spar	spar at taper	Sheet: 3/16" spruce		Laser	2	
19	2nd endspars	spar at taper	Sheet: 3/16" spruce		Laser	2	
20	taper front spar	horizontal front spar for taper leading edge	Sheet: 3/16" spruce		Laser	2	
21	3rd endspar	spar at taper	Sheet: 3/16" spruce		Laser	2	
22	4th end spar cap	spar at taper	Sheet: 3/16" spruce		Laser	2	
23	airfoil aileron joiners	airfoils in front of aileron with cut in middle for "joiner"	Sheet: 1/4" balsa		Laser	4	
24	mounting block	block to drop screw into	3/4" balsa stick	3/4" x 3/4" x 3"	Hack saw	4	
25	airfoil aileron 2nd to end	tranistional airfoil near taper to support taper spars	Sheet: 1/4" balsa		Laser	4	
26	airfoil aileron straight end cap	tranistional airfoil near taper to support taper spars (right before taper)	Sheet: 1/4" balsa		Laser	2	
27	winglet	Winglet	Sheet: 1/4" balsa		Laser	2	
28	reinforce	between mounting blocks to reinforce "mate plate" and "airfoil linkage" connection	stick wood	1/4 height x (.25-.5) x 9.5"	hack saw	2	
29	web	creates "I beam" for spars	Sheet: 1/4" balsa		Laser	26	
30	servo bottom mount wing	servo bottom mount	Sheet: 1/4" balsa		Laser	2	
31	servo side wing	servo side mount	Sheet: 1/4" balsa		Laser	2	
32	ServoSupport wing	servo screw on mount (detachable)	Sheet: 1/4" balsa		Laser	2	
33	Servo					2	

Monokote: .5" or more overhang included in dimensions below

Color	Dimensions	Qty	purpose	Done
Gold	19.25 x 57.25	2	main top	
Blue	12 x 18.5	6	bottom	
silver	12x18.5	4	bottom	
Black	22x12.5	4	taper	
Black	24x8	1	center	

1/32" Balsa leading edge sheeting

Place	Dimensions	qty	notes
bottom sheeting inside	4.22 x 37.625	2	1 stock sheet
top sheeting inside	4.32 x 37.625	2	1 stock sheet
bottom sheeting outside	4.22 x 18.875	2	1/2 stock sheet
top sheeting outside	4.32 x 18.875	2	1/2 stock sheet

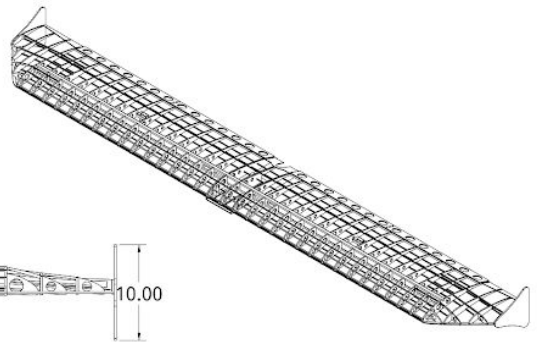

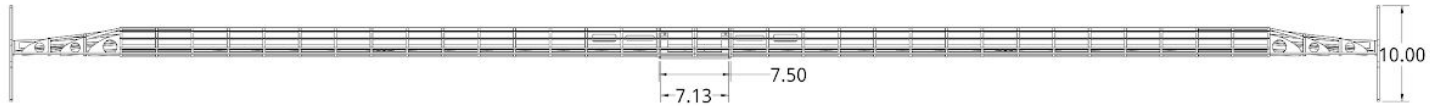

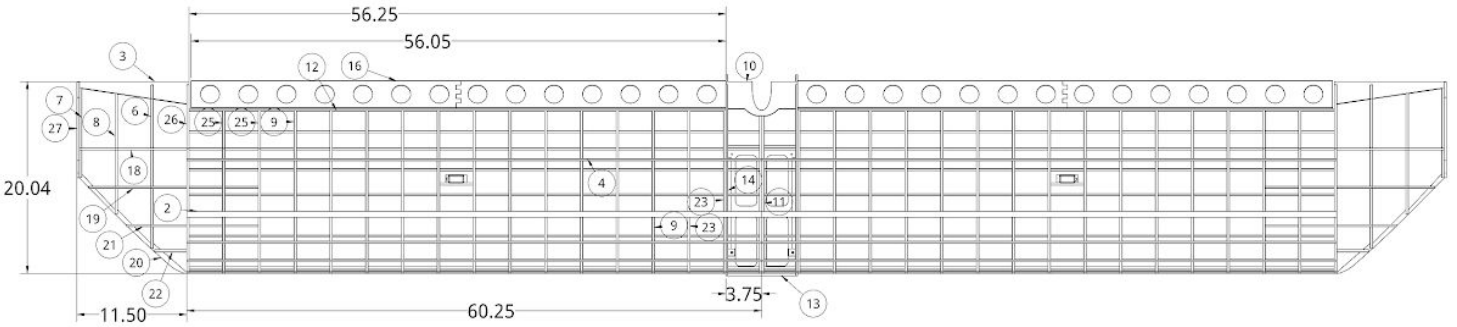

Dwg Name	Wing
Engineer	Ryan Ogilvie
Date	28 Jan 2018
Size	D
Scale	1:8
Sheet	1 of 1
Rev	A

ITEM NO.	PART NUMBER	DESCRIPTION	STOCK	FINAL DIMENSIONS	MANUFACTURING	QTY.	DONE?
1	Mount	Middle plate to mount everything too	1/4" Spruce sheet		Laser	1	
2	LeadingEdge-1	leading edge spar	Balsa stick 1/4x 1/4	1/4" x 1/4" x 34.5"	Hack saw	2	
3	TrailingEdge	Trailing edge spar mount to elevator	Balsa stick	1/2" x .41" x 34.5"	Table Saw/ Hack Saw	2	
4	HorzProfile	Main airfoil profile	1/4" Balsa Sheet		Laser	18	
5	TopSpar	support Spars for horizontal	.5" x .25" Spruce stick	1/2" x 1/4" x 69"	Table Saw/ Hack saw	2	
6	ServoSupportL	Servo mount	3/16" spruce Sheet		Laser	2	
7	MountSpacer	mount plate to tube spacer	spruce stick	.5" x (3/4" x 3/4")(ish)	Hack Saw	4	
8	ElvToHorz	Elevator Spar	Stick balsa or spruce	3/8" x 3/8" x 32"	Table Saw/ Hack Saw	2	
9	ElvSheetingTry1	Elevator Sheeting	1/16" Balsa Sheet		Laser	4	
10	ElvRib	Elevator Rib	1/4" Balsa Sheet		Laser	24	
11	VerticalToRudder	Vertical trailing edge mount to rudder	Balsa stick	1/2" x 1/2" x 27.5"	Table Saw/Hack saw	1	
12	VerticalLeadingEdge	Vertical leading edge	Balsa Stick 1/4 x 1/4	1/4" x 1/4" x 24.75"	Hack saw	1	
13	vert profile	Vertical airfoil profile	1/4" Balsa Sheet		Laser	7	
14	vert spar	support spars vertical	Spruce Stick .5" x .25"	1/2" x 1/4" x 25.16"	Table saw/ Hack saw	2	
15	RudderContorlSurfToRuder1	Rudder spar	stick balsa or spruce	3/8" x 3/8" x 27.5"	Table saw/ hack saw	1	
16	RudderProfile1	rudder rib	1/4" Balsa Sheet		Laser	18	
17	RudderSheeting	Rudder sheeting	1/16" Balsa Sheet		Laser	2	
18	Tactic TSX57	Servo	Servo		self tapping screws	3	
19	plate to rudder seat	Plate between mount and vertical	1/4" Balsa Sheet		Laser	1	
20	HorzProfile center	Airfoil over mount plate	1/4" Balsa Sheet		Laser	2	
21	rudder brace	angle brace for under mount to vertical	1/4" Spruce Sheet		Laser	1	

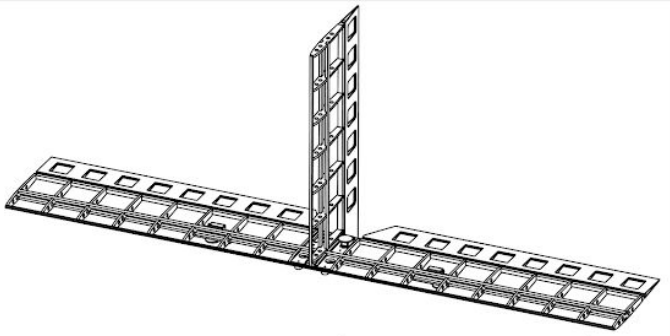

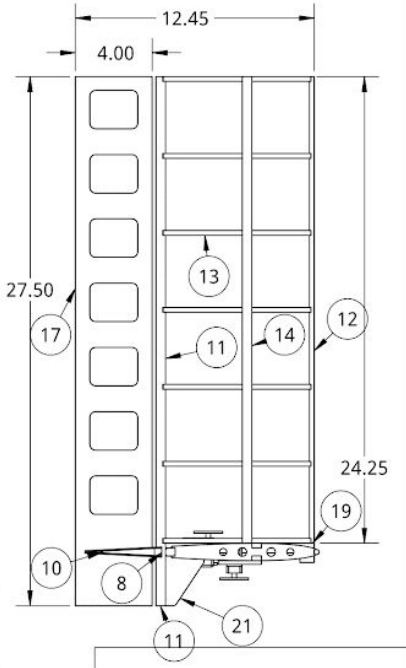

Glue Vertical First, then place on horizontal and glue rest together

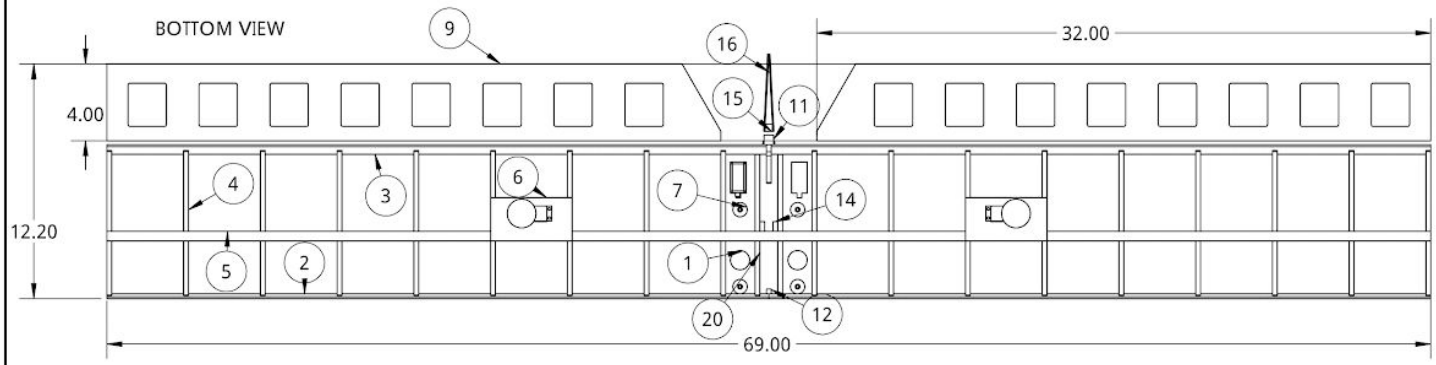

TITLE:

SIZE	DWG. NO.	REV
B	Horizontal	
SCALE: 1:6	WEIGHT:	SHEET 1 OF 1

ITEM NO.	PART NUMBER	DESCRIPTION	STOCK	FINAL DIMENSIONS	MANUFACTURING	QTY.	Done?
1	double boom 2.0	Main Support boom	Poplar or spruce stick	3/4" x 3/4" x 47"	tablesaw/hacksaw	1	
2	balsa material for ball side 2.0	back balsa piece	1/4" balsa sheet		Laser	2	
3	battery box half tapper	front side plate holds battery plate	1/4" spruce sheet		Laser	2	
4	front plate prop attach	Front plate motor attach	1/4" spruce sheet		Laser	1	
6	second half of tapper	front side plate tapered	1/4" balsa sheet		Laser	2	
7	tapper betweens	bottom sticks under taper	balsa or spruce stick	(1/4" x 1/4") (ish) x 7"	hacksaw	3	
8	side of luggage compart 2.0	luggage ball side plate	1/4" spruce sheet		Laser	2	
9	end plate for weight compart 2.0	weight front plate	1/4" spruce sheet		Laser	1	
10	battery box slid door	battery door	1/4" balsa sheet		Laser	1	
11	bottom of weight compartment 4.0	weight bottom support	.205" ply sheet		Laser	1	
12	floor for balls 4.0	Floor holding balls	1/8" balsa sheet		Laser	1	
13	end for balls (door)	Ball door	1/4" balsa sheet		Laser	1	
14	front plate for balls 4.0	Front of ball compartment	1/8" spruce sheet		Laser	1	
15	end for slider compart	weight door	1/4" balsa sheet		Laser	1	
16	front plate prop supprt	front plate reinforcements	stick spruce	3/4" x 3/4" x 3/4" block	chopsaw	4	
17	top cover for t ball	cover for balls before wing	1/4" balsa sheet		Laser	1	
18	battery bottom	battery holding plate	.205" ply sheet		Laser	1	
20	latch2	latch for doors	latch		Glue	3	

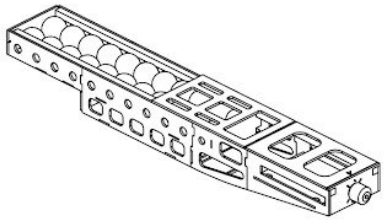

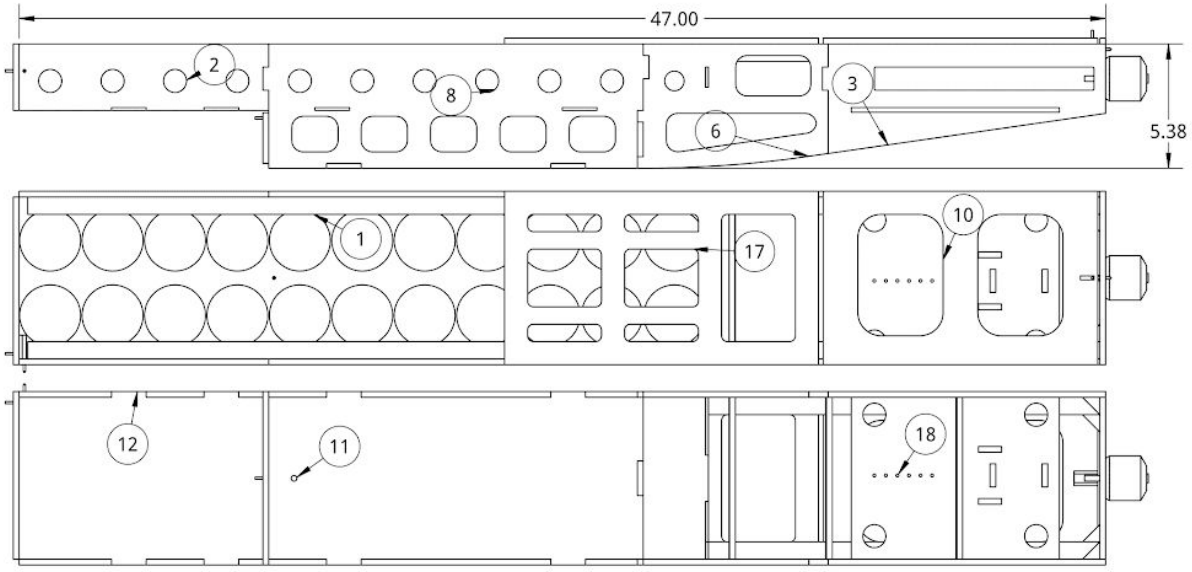

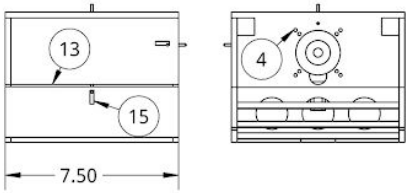

SIZE	DWG. NO.	REV
B	New Fuselage	
SCALE: 1:5	WEIGHT:	SHEET 1 OF 1

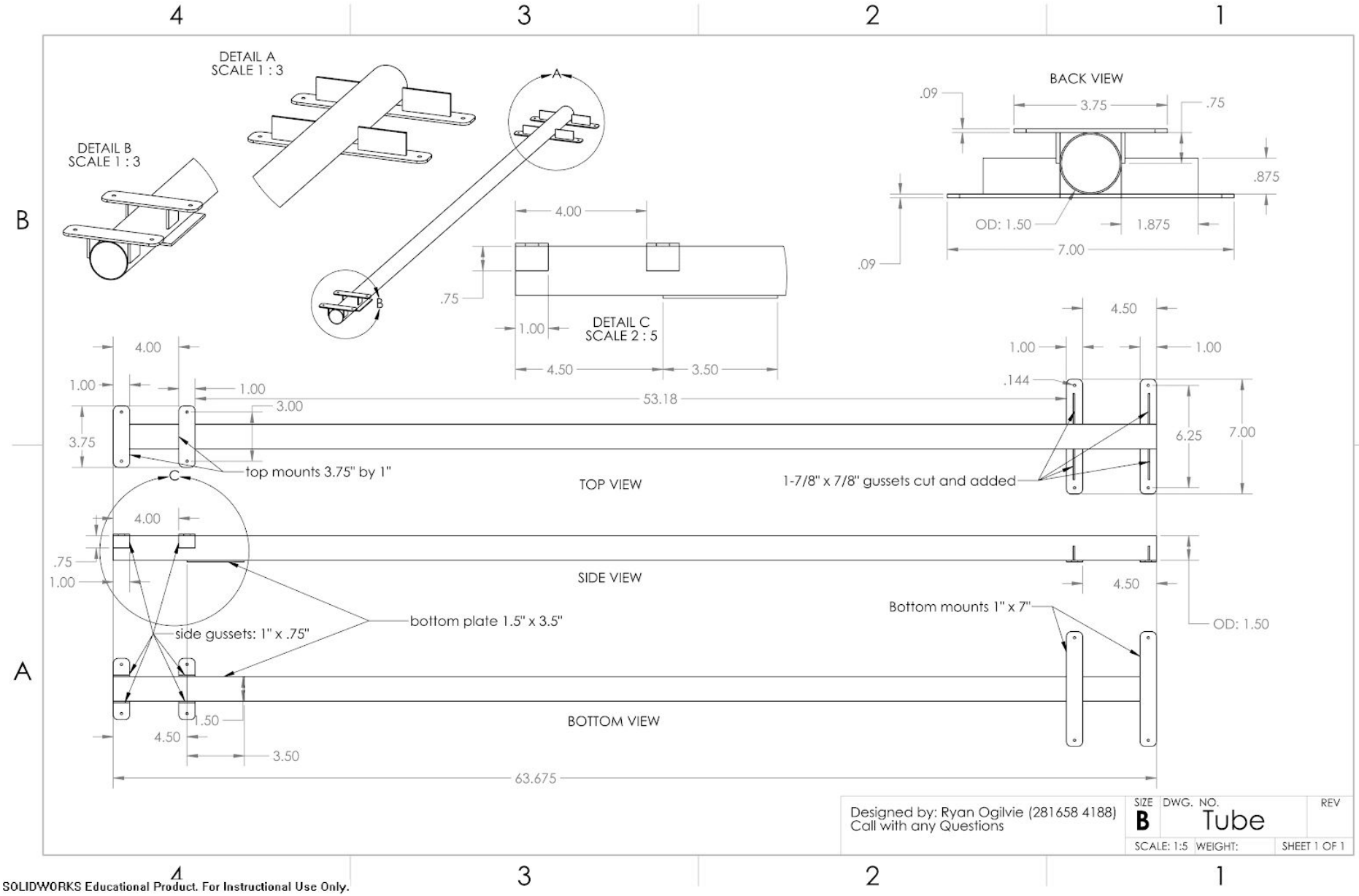

Designed by: Ryan Ogilvie (281658 4188)
Call with any Questions

SIZE	DWG. NO.	REV
B	Tube	
SCALE: 1:5	WEIGHT:	SHEET 1 OF 1

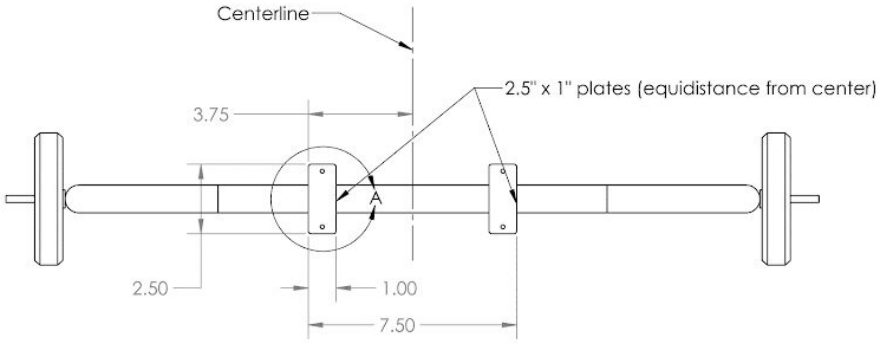

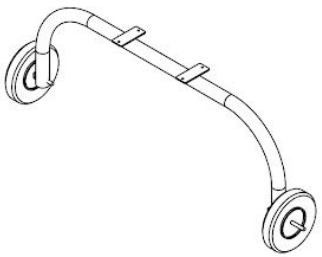

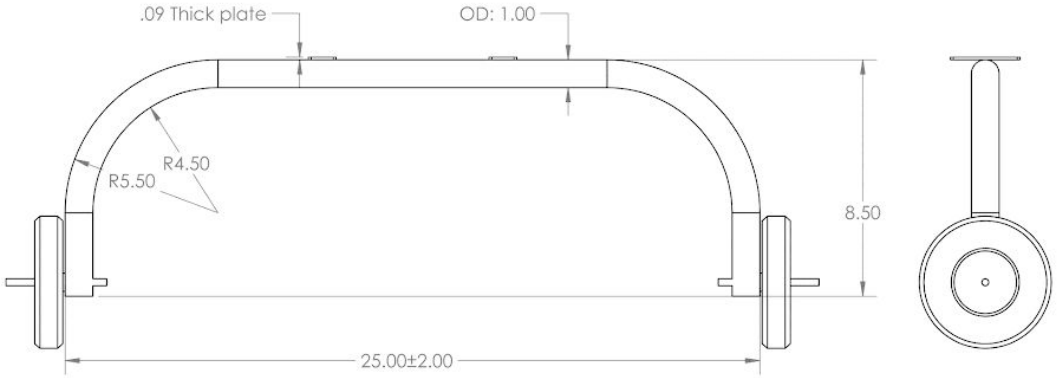

Designed by: Ryan Ogilvie (281658 4188) Call with any Questions	SIZE B	DWG. NO. MountingRound	REV A
	SCALE: 1:4	WEIGHT:	SHEET 1 OF 1

A5: Photo Gallery

Figure A.5.1: Safety Inspections

Figure A.5.2: First Test Flight

Figure A.5.3: Competition Flight

Figure A.5.4: Lining up for flight

Figure A.5.5: First Test Flight Take-Off

Figure A.5.6: Awards Ceremony

Photo A.5.7: Team Photo

A6: Specifications

This is a simplification of the requirements and limitations laid out in the SAE rules.

Table A.6.1: Competition Specifications

Wattage	< 1000 Watts
Size	< 12ft wingspan (only requirement)
Battery	22.2V lithium polymer (LiPo), Min: 3000mah
Takeoff	< 200ft
Flight Circuit	1 Loop
Max Weight	55 pounds
Motor	Electric
Materials	No fiber reinforced plastics

These are the engineering specifications of the 2018 plane compared with the specifications for the 2017 plane.

Table A.6.2: Engineering Specifications

	2018 Plane	2017 Plane
Plane Weight	17 lbs	15 lbs
Wing area	19.2 ft^2	13.3 ft^2
Max weight	31.7 lbs	24 lbs
Carried weight	14.7 lbs	9 lbs
Score	68.7	24.5 (max) 14.8 (avg)
Tennis balls carrying	22	15 (max)
Cargo carrying	11 lbs	7.5 lbs (max)

A7: Propeller Test Data

Here is a table of the propeller test data. Predictions were made using the method in section 7 for static thrust without a limiter.. Limiter is set to 1000 watts.

Table A.7.1: Competition Specifications

		Prediction w/o limiter		Actual w/o limiter		Actual with limiter	
Motor (KV)	Propeller	Watts	Force	Watts	Force	Watts	Force
450	14x7E	772	7	655	6.9	623	7.4
450	15x8E	1123	9.5	850	8.45	835	9.2
450	16x8E	1408	11.9	1190	11.1	956	10.3
500	14x7E	990	8.6	970	8.7	893	9.1
500	15x8E	1541	11.7	1450	12.3	942	9.6
260	21x13E	1457	13.1	1410	15.9	969	13.5
260	20x10W	828	9.7	1293	15.9	937	14.1
260	20x10E	828	9.7	1111	14.8	890	13.7

A8: Boom Test

The original plane design included two wooden booms connecting the wing and tail. A preliminary boom test was performed on the two wood boom design. This test was performed to analyze the amount of deflection the booms would experience under normal flight loads. A torque load was applied using an extension arm and weights, as shown in Figure A.8.1. The weights were moved to various distances using C Clamps to vary the applied torque. It was quickly determined the amount of deflection was too great for flight stability and another boom design would need to be pursued.

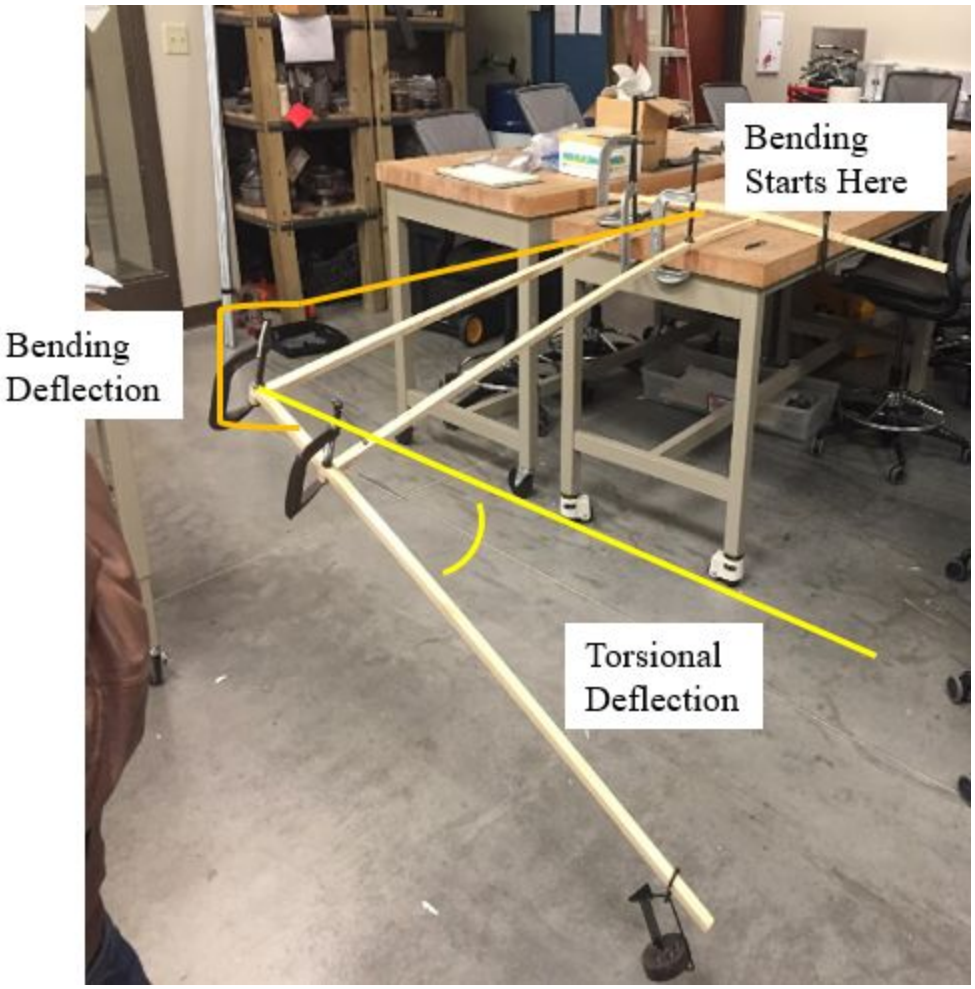

Figure A.8.1: Testing Setup and Deflection Definitions

Table A.8.1: Deflection Test Data

Torque (lb-in)	Bending Deflection (in)	Torsional Twist(deg)
0	1	6.79
22	1.75	10.91
39	1.75	13.78
67	1.75	19.36
90	1.75	22.65
112	1.75	26.46

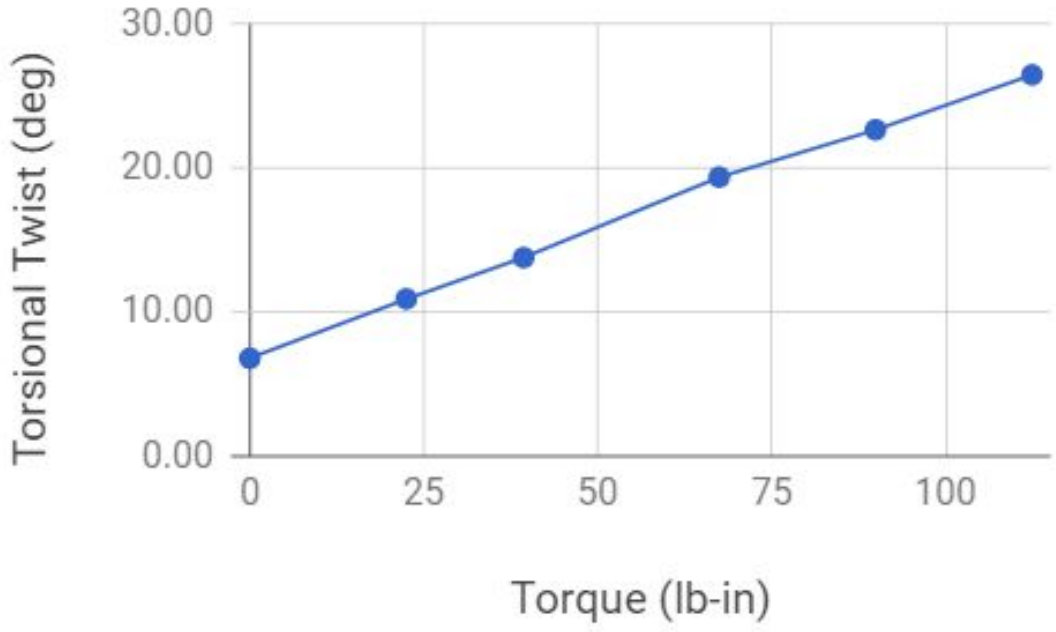

Figure A1: Deflection vs Weight Position

A9: Landing Gear - Structural Analysis Calculations

The landing gear was modeled as a straight piece of tube experiencing bending and torsion. The dimensions are shown below.

OD	1	in
Wall t	0.095	in
Area	0.270	in^2

Shear was calculated with force divided by area, with an impact force of 100 lbs. This was applied to one section to simulate a rough landing. In an ideal landing, this would be applied to both sides of the landing gear.

Area	0.270	in^2
F	100	lbs
σ (P/A)	370.42	psi

Bending was calculated with MC/I using the values shown below.

F	100	lbs
distance	12	in
M	1200	in lbs

c	0.5	in
I	0.027943	in^4
σ (MC/I)	21472	psi

The sum of the stresses and calculation of safety factor is shown below.

Shear Stress on Cross Section	370.4	psi
Bending Stress at Center	21473	psi
Von Mesis Equivalent	21476	psi
6061 Aluminum Yield Strength	30000	psi
Factor of Safety	1.40	

A10: Tail - Structural Analysis Calculations

Bending was considered the most critical load on the wing and horizontal stabilizer. From CFD Analysis, the distributed load on the tail was 6.89 lbs.

Load	6.89	lbs
Length	2.75	ft
Bending Moment	18.949	ft lbs
	227.34	in lbs

The spar dimensions are shown below. The spars are assumed to carry all the loading. Parallel axis theorem is used to find the moment of inertia for the combined spars.

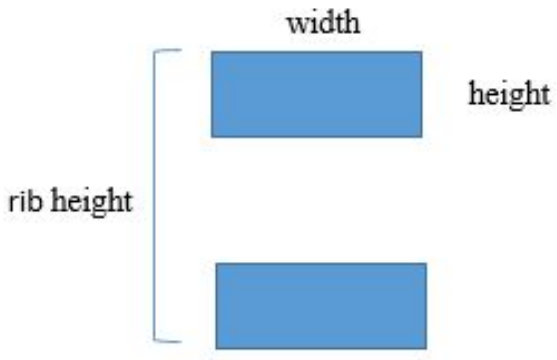

width	0.500	in
height	0.250	in
Icentroid	0.001	in^4
Area	0.125	in^2
rib height	0.908	in
d	0.454	in
I total for 1 stringer	0.026	in^4
I total both stringers	0.053	in^4

The bending stress and safety factor are shown below.

Bending Stress (MC/I)	1953.6	psi
Spruce Yield Strength	10,200	psi
FS	5.22	

This is a high factor of safety, chosen due to availability and reduced deflection. Deflection with this size is extremely small. The wing analysis follows the same calculation procedure.

Deflection	PL^3/3EI	
	0.000687	in

A11: Tube - Structural Analysis Calculation

The tube experiences several types of loading. The dimensions and moments of inertia are shown below.

Outer Diameter	1.375	in
Thickness	0.035	in
I	0.033076	in^4
J	0.066153	in^4

The bending stress calculations are shown below. The loads are derived from fluid analysis, as discussed in Section 8: Loading and Environmental Assumptions.

Elevator Bending		
Load	2.865	lb
Distance	54	in
Moment	154.71	lb in
σ (MC/I)	3215.68	psi

Weight Bending		
Load	2.00	lb
Distance	54	in
Moment	108	lb in
σ (MC/I)	2244.80	psi

Rudder Bending		
Load	1.91	lb
Distance	54.00	in
Moment	103.33	lb in
σ (MC/I)	2147.82	psi

There is torsion present due to rudder force acting above the plane of the tube.

Torsion Rudder		
Load	2.00	lb
Radius	18	in
Torque (Tc/J)	12.57	lb in
σ	130.635	psi

These von mesis equivalent of these stresses leads to a high factor of safety.

VM Equivalent Stress	4473	psi
Yield Strength of 6061 Aluminum	40000	psi
Factor of Safety	8.9	

Two types of deflection were calculated: cantilever beam deflection and torsional deflection.

P (Force)	6.7786	lb
E (Elastic Modulus)	10000000	psi
L (Length)	54	in
I (Moment of Inertia)	0.033076	in^4
Beam Deflection (Pl^3/3EI)	1.075677	in

Torque	12.57	ft lb
Length	4.5	ft
thickness	0.035	in
Outer Diameter	1.5	in
c	0.75	in
Inner Diameter	1.43	in
Angle of Twist (radians) (Tc/JG)	1.37E-02	rad
Angle of Twist (degrees)	0.78	deg

A12: Mathematica Code for Determining Weight Capacity of a Sample Wing

In[349]:=

```
Clear["Global`*"]

cl = 1.571; (* maximum lift coefficient *)
cl0 = 0.783; (* lift coefficient at zero degrees angle of attack *)
cdInit = 0.17; (* average drag coefficient between 0 and vCut *)
Crr = 0.112; (* drag coefficient for wheel deflection *)
A = 1.104; (* wing planform area, m^2 *)
ToffLimit = 61; (* takeoff distance allowed, meters *)
vCut = 4.5; (* velocity where drag coefficent vs velocity curve
 becomes linear, m/s *)
mInc = 0.05; (* mass increment per iteration, kg *)
p = 1.225; (* density of air, kg/m^3 *)
t = .01(* time step, seconds *);
```

In[353]:=

```
(* describing the linear portion of the drag coefficient vs velocity
 curve *)
v1 = 15;
cd1 = 0.049;
v2 = vCut;
cd2 = 0.058;
```

In[357]:=

```
slope = (cd1 - cd2) / (v1 - v2);
b = cd1 - slope * v1;
cd[v_] = slope * v + b
```

Out[359]=

$$0.0618571 - 0.000857143\, v$$

```
(* propellor parameters, inches *)
pitch = 10;
diam = 20;

(* conversion factors *)
kgTolb = 2.20462;
msTomph = 2.23694;
mToft = 3.28084;
inmToms = 0.000423333;

(* propellor thrust equation, Newtons, where v = plane velocity *)
F[v_] =
  1.10 * (4.292399 * 10^-8 * RPM * diam^3.5 / Sqrt[pitch] *
     (4.23333 * 10^-4 * RPM * pitch - v));

(* setting the wattage used at static thrust to 1000 and solving for RPM *)
Sol1 = Solve[RPM * pitch * inmToms * F[0] == 1000, RPM];
RPM = RPM /. Sol1[[3]]
```

Out[369]=

```
4709.55
```

```
(* velocity after undergoing time step t, m/s *)
V[v_, CL_, m_] =
  v + ((F[v] - ((.5 * cd[v] * p * A * v^2) + (L - .5 * p * A * CL * v^2) * Crr)) / m) * t;

(* acceleration at current time step m/s^2 *)
a[v_, CL_, m_] = (F[v] - ((.5 * cd[v] * p * A * v^2) + (L - .5 * p * A * CL * v^2) * Crr)) / m;

(* initializing parameters. X = distance traveled (meters),
v = velocity (m/s), m = mass (kg) *)
X = 0;
v = 0;
m = 1;
```

In[373]:=

```
(* solving for takeoff weight capacity *)
While[X < ToffLimit, X = 0;

 v = 0; L = m * 9.81; ToV = Sqrt[L / (.5 * cl * A * p)];

 While[v < vCut,
  X =
   X + v * t +
    .5 * ((F[v] - ((.5 * cdInit * p * A * v^2) + (L - .5 * p * A * cl0 * v^2) * Crr)) / m) *
     t^2;

  v = v + ((F[v] - ((.5 * cdInit * p * A * v^2) + (L - .5 * p * A * cl0 * v^2) * Crr)) / m) * t];

 While[v < ToV, X = X + v * t + .5 * a[v, cl0, m] * t^2; v = V[v, cl0, m]];
 m = m + mInc;]

mTakeoff = (m - mInc) * kgTolb;

Print[mTakeoff " lbs"];
```

```
31.1954 lbs
```

Takeoff Weight

In[376]:=

```
Clear[v];
(* solving for velocity vCrit where thrust = drag *)
vCrit = Solve[F[v] == 0.5 * p * A * cd[v] * v^2, v];

Lmaintain = 0.5 * p * cl0 * A * v^2 /. vCrit[[2]];

Print[v * msTomph /. vCrit[[2]], " mph"]

mMaintain = (Lmaintain / 9.81) * kgTolb;

(* in-flight weight capacity *)
Print[mMaintain " lbs"]
```

```
36.82 mph
32.2374 lbs
```

In-Flight Weight

In[382]:=

```
(* calculating takeoff distance using in-flight weight *)
X = 0;
v = 0;
m = Lmaintain / 9.81;
While[v < vCut,
 X =
  X + v * t +
   .5 * ((F[v] - ((.5 * cdInit * p * A * v^2) + (L - .5 * p * A * cl * v^2) * Crr)) / m) * t^2;
 v = v +  ((F[v] - ((.5 * cdInit * p * A * v^2) + (L - .5 * p * A * cl * v^2) * Crr)) / m) * t]
```

In[383]:=

```
While[v < ToV, X = X + v * t + .5 * a[v, cl0, m] * t^2; v = V[v, cl0, m]]
Print[X * mToft, " ft"]
```

```
207.982 ft
```

Could take off in this distance at in-flight weight

In[385]:=

```
(* determining whether in-
 flight or takeoff weight capacity is the limitnig weight *)
lWeight = If[mMaintain > mTakeoff, " Takeoff " mTakeoff, " In-flight " mMaintain];

Print[lWeight]
```

```
31.1954  Takeoff
```

Limiting Weight